External dc bias-field effects in the nonlinear ac stationary response of dipolar particles in a mean-field potential

Nijun Wei,[1] Pierre-Michel Déjardin,[2] Yuri P. Kalmykov,[2] and William T. Coffey[1]
[1]*Department of Electronic and Electrical Engineering, Trinity College, Dublin 2, Ireland*
[2]*Laboratoire de Mathématiques et de Physique (LAMPS, EA4217), Université de Perpignan Via Domitia, F-66860, Perpignan, France*
(Received 11 February 2016; published 14 April 2016)

External dc bias-field effects on the nonlinear dielectric relaxation and dynamic Kerr effect of a system of permanent dipoles in a uniaxial mean-field potential are studied via the rotational Brownian motion model postulated in terms of the infinite hierarchy of differential-recurrence equations for the statistical moments $f_n(t) = \langle P_n \rangle(t)$ (the expectation value of the Legendre polynomials P_n). By solving these equations, the nonlinear dielectric and Kerr-effect ac stationary responses are evaluated for arbitrary dc field strength via perturbation theory in the ac field. Simple analytic equations based on the large separation of the time scales of the fast intrawell and slow overbarrier (interwell) relaxation processes are also derived.

DOI: 10.1103/PhysRevE.93.042208

I. INTRODUCTION

The theory of electric polarization of dielectric fluids is essential for understanding dielectric and electro-optical relaxation phenomena. This problem was originally treated by Debye [1], who calculated the linear dielectric susceptibility of noninteracting polar molecules subjected to a weak ac electric field $\mathbf{E}(t) = \mathbf{E}\cos\omega t$ using the rotational diffusion model when inertial effects are negligible and the rotation of the molecule can be described by a random walk over small angular orientations. Now, in the linear response, the complex dielectric susceptibility is independent of the electric field strength $\mathbf{E}$ so that the orientational electric polarization of noninteracting permanent dipoles in an ac field $\mathbf{E}(t)$ depends solely on the first-order Legendre polynomial averaged over dipole orientations $\langle P_1(\cos\vartheta)\rangle(t)$, ϑ being the polar angle of the electric dipole moment vector $\boldsymbol{\mu}$ of the molecule. Later, the original Debye calculation was generalized using perturbation theory to nonlinear phenomena in polar dielectrics subjected to strong external fields [2–4]. In particular, we cite the dynamic Kerr-effect response governed by the averaged second-order Legendre polynomial $\langle P_2(\cos\vartheta)\rangle(t)$ and the nonlinear dielectric effect [2–6]. The conclusions for the Kerr-effect relaxation in a pure sinusoid electric field are that the square law nonlinearity rectifies $\mathbf{E}(t)$, yielding a frequency-dependent dc response superimposed on the dephased second harmonic [2]. In the nonlinear dielectric relaxation, additional terms in the fundamental, third, etc., harmonic appear in $\langle P_1(\cos\vartheta)\rangle(t)$ [3–5]. These nonlinear effects have been confirmed by experimental data (e.g., see Refs. [2,7–10]). Additionally, the Debye theory has also been extended to nonlinear effects in dipolar systems in arbitrarily large external fields (see, for example, Refs. [11–16] and references cited therein). Nevertheless, these calculations still assume assemblies of noninteracting dipoles implying that the Debye model and its extensions may not be used for dense dipolar systems, where intermolecular interactions occur. However, experimental data of such dipolar systems may be explained using a more sophisticated model of the noninertial rotational Brownian motion of dipoles in an external mean-field potential V (e.g., see Refs. [17–19]).

In particular, this mean-field approximation was used to treat nematic liquid crystals in Refs. [17,18], where the linear dielectric response was calculated via the rotational Brownian motion in the Maier-Saupe uniaxial anisotropy potential:

$$V = -K\cos^2\vartheta. \tag{1}$$

Here K is the anisotropy constant and ϑ is the colatitude, i.e., the angle between $\boldsymbol{\mu}$ and the Z axis of the laboratory coordinate system. The mean-field approximation has a restricted applicability because it ignores local order effects. Nevertheless, it is easily visualized and permits quantitative evaluation of dielectric parameters, demonstrating the effect of intermolecular interactions on dielectric parameters that must be accounted for to compare with experiments [20]. Now, the theory of dielectric relaxation of nematic liquid crystals bears a close resemblance to the theory of magnetic relaxation of single domain ferromagnetic particles as formulated by Brown [21]. Brown's major contribution to this theory was the derivation of the Fokker-Planck equation for the distribution function of the particle magnetic moment orientations on the unit sphere. For the longitudinal relaxation in uniaxial magnetic nanoparticles, this Fokker-Planck equation becomes mathematically identical to that used in the theory of dielectric relaxation of nematic liquid crystals [16]. Various numerical methods have also been developed [22,23] for calculating the nonlinear ac stationary response of dipolar molecules (electric dipoles) in the Maier-Saupe uniaxial potential, Eq. (1), and for that of uniaxial magnetic nanoparticles (magnetic dipoles), which, in most respects, is just a replica of dielectric relaxation of nematics. Such numerical approaches cannot yield, however, simple formulas for comparison with experiments and the qualitative behavior of the nonlinear response is not obvious. Preliminary steps toward an accurate analytical treatment of nonlinear response of dipoles in the uniaxial potential, Eq. (1), were made in Refs. [24,25], showing that the nonlinear response to an ac driving field $\mathbf{E}(t)$ can be evaluated by utilizing the so-called two-mode approximation [16,26,27] combined with Morita's treatment [28] of the nonlinear response of dipolar systems, whereby the distribution function induced by an external perturbing field may be calculated from the appropriate Green function in the absence of the perturbation, with the linear response theory as a special case. Thus, the *linear* response of dipoles in a mean-field

potential comprising an infinity of relaxation modes may be accurately represented by two modes only [16,26,27], namely, a slowest interwell barrier crossing mode and a fast mode, representing the infinity of high-frequency near-degenerate "intrawell" modes approximated as a single mode. Here we generalize this approach [24–27] to include the effects of an external dc bias field on the *nonlinear* ac stationary response of a system of permanent dipoles in the uniaxial mean-field potential, Eq. (1). Both matrix perturbation and analytical solutions are given for the ac stationary response of the first- and second-rank response functions $\langle P_1(\cos\vartheta)\rangle(t)$ and $\langle P_2(\cos\vartheta)\rangle(t)$, determining the nonlinear dielectric and Kerr-effect responses. Our calculations are, in particular, motivated by recent measurements of the nonlinear frequency-dependent polarization response in strong dc electric fields [29], where the influence of the dc field on the glass temperature T_g of glycerol was demonstrated, showing that the T_g increase is in proportion with the square of the dc field amplitude. Here an accurate representation of the nonlinear components of the ac stationary dielectric response spectrum is required in order to compare with experimental data [29,30].

II. BASIC RELATIONS

We shall consider the nonlinear ac stationary response of rigid dipolar particles undergoing rotational Brownian motion in a mean-field potential, Eq. (1), acted on by strong external superimposed dc $\mathbf{E}_0$ and ac $\mathbf{E}(t) = \mathbf{E}\cos\omega t$ fields. Each particle contains a rigid dipole $\boldsymbol{\mu}$. For simplicity we suppose that both $\mathbf{E}_0$ and $\mathbf{E}$ are directed along the Z axis of the laboratory coordinate system and that effects due to the anisotropy of the polarizability of the particles can be neglected. The calculation of the nonlinear ac stationary response of permanent dipoles to an ac driving field usually starts with the rotational diffusion or Smoluchowski equation for the distribution function $W(\boldsymbol{\mu},t)$ of orientations of dipole moments $\boldsymbol{\mu}$ on the surface of the unit sphere under the influence of external electric fields [16], viz.,

$$\frac{\partial W}{\partial t} = L_{\mathrm{FP}}W + L_t W, \tag{2}$$

where

$$L_{\mathrm{FP}}W = (2\tau_D)^{-1}[\Delta W + \beta\nabla\cdot(W\nabla V)] \tag{3}$$

is the unperturbed Fokker-Planck operator, which contains the effect of the potential V due to the mean field and the time-independent dc bias field, while

$$L_t W = (2\tau_D)^{-1}\beta\nabla\cdot(W\nabla V_t)$$

contains the effect of the time-dependent potential V_t due to the ac field $\mathbf{E}(t)$. Here ∇ and Δ are the gradient and Laplacian on the surface of the unit sphere, respectively, τ_D is the free diffusion relaxation time, and $\beta = (kT)^{-1}$ is the inverse thermal energy. When the superimposed effective field (due to the uniaxial anisotropy) and external dc bias field $\mathbf{E}_0$ are directed along the Z axis of the laboratory coordinate system, the axially symmetric potential $V(\vartheta)$ is given by

$$\beta V(\vartheta) = -\sigma\cos^2\vartheta - \xi_0\cos\vartheta, \tag{4}$$

where $\sigma = \beta K$ is the dimensionless anisotropy or inverse temperature parameter (K is the anisotropy constant) and $\xi_0 = \beta\mu E_0$ is the dimensionless dc bias field parameter. The time-dependent ac field is assumed to be parallel to the dc bias field so that

$$\beta V_t(\vartheta,t) = -\xi\cos\vartheta\cos\omega t, \tag{5}$$

where $\xi = \beta\mu E$ is the dimensionless ac field parameter. The uniaxial potential Eq. (4) has two nonequivalent wells with minima at $\vartheta = 0$ and π separated by a barrier at $\vartheta_0 = \arccos(-\xi_0/2\sigma)$. For a positive, finite dc field, $\xi_0 > 0$, the dipoles in the shallower well at $\vartheta = \pi$ are inhibited from crossing into the deeper well by the potential barrier of height $\sigma(1-\xi_0/2\sigma)^2$. However, the dipoles populating the deeper well at $\vartheta = 0$ have smaller probability to escape from the well, owing to the elevated potential barrier height $\sigma(1+\xi_0/2\sigma)^2$. Thus, the escape rate strongly depends on the dc field strength, which affects the orientational relaxation and, hence, the dielectric and Kerr-effect responses.

For the axially symmetric potential Eq. (4), the azimuthal angle dependence of the distribution function W may be ignored. Hence, $W(\vartheta,t)$ can be expanded in a Fourier series as [2–5,16]

$$W(\vartheta,t) = \sum_{n=0}^{\infty}(n+1/2)f_n(t)P_n(\cos\vartheta), \tag{6}$$

where $P_n(z)$ is the Legendre polynomial of order n [31] and the Fourier coefficients (relaxation functions) $f_n(t)$ are formally given by

$$f_n(t) = \int_0^{\pi} P_n(\cos\vartheta)\,W(\vartheta,t)\sin\vartheta\,d\vartheta, \tag{7}$$

due to the orthogonality property of the Legendre polynomials, viz.,

$$\int_0^{\pi} P_n(\cos\vartheta)\,P_m(\cos\vartheta)\sin\vartheta\,d\vartheta = \frac{2\delta_{nm}}{2n+1} \tag{8}$$

(δ_{nm} is Kronecker's delta). On substituting Eq. (6) into the Fokker-Planck equation (2) and utilizing the properties of the Legendre polynomials, we obtain an infinite hierarchy of differential-recurrence equations for the relaxation functions $f_n(t)$, $n = 1,2,\ldots$, namely,

$$\begin{aligned}\tau_D\frac{d}{dt}f_n(t) + c_n f_{n-2}(t) + d_n f_n(t) + g_n f_{n+2}(t)\\ = a_n(\xi_0 + \xi\cos\omega t)[f_{n-1}(t) - f_{n+1}(t)],\end{aligned} \tag{9}$$

where the coefficients a_n, c_n, d_n, and g_n are given by

$$\begin{aligned} a_n &= \frac{n(n+1)}{2(2n+1)}, \quad c_n = -\frac{\sigma n(n^2-1)}{4n^2-1},\\ d_n &= \frac{n(n+1)}{2} - \frac{\sigma n(n+1)}{(2n-1)(2n+3)},\\ g_n &= \frac{\sigma n(n+1)(n+2)}{(2n+3)(2n+1)}. \end{aligned}$$

Our goal is to evaluate, by solving Eq. (9), the ac stationary response of the electric polarization $P(t)$ and dynamic Kerr-effect $K(t)$ ac stationary responses [1,2], which are

defined as

$$P(t) = b_1\langle P_1(\cos\vartheta)\rangle(t) = b_1 f_1(t) \tag{10}$$

and

$$K(t) = b_2\langle P_2(\cos\vartheta)\rangle(t) = b_2 f_2(t), \tag{11}$$

where the coefficients b_1 and b_2 depend on the concentration of polar particles, particle depolarization factors, the relative permittivity, and other parameters. Here, for simplicity, we assume that $b_1 = 1$ and $b_2 = 1$, i.e., we consider normalized responses only. Furthermore, we suppose that the internal field effects and the long-range torques due to the connection between the dipole moments and the Maxwell fields may be ignored. In the dynamic nonlinear response, these effects present a very difficult problem. However, in the first approximation they may be ignored for dilute systems. Here the internal field effects (the effects of long-range torques due to the connection between the average moments and the Maxwell fields) are not taken into account.

III. MATRIX PERTURBATION SOLUTION

Now, although the applied ac electric field in experiments [7–10] can be high enough ($\geqslant 10^6$ V/m) to observe nonlinear effects, the energy of the dipole in the field $|V_t|$ remains sufficiently weak compared to the thermal energy to allow one to use perturbation theory in the calculation of the ac stationary response for a weak ac field $\xi(t) = \xi\cos\omega t$ ($\xi \ll 1$). Thus, we may seek perturbation solutions of Eq. (9) in the form

$$f_n(t) = f_n^{(0)} + f_n^{(1)}(t) + f_n^{(2)}(t) + f_n^{(3)}(t) + \cdots, \tag{12}$$

where $f_n^{(m)} \propto \xi^m$, yielding the coupled differential-recurrence relations

$$\begin{aligned}\tau_D\frac{d}{dt}f_n^{(m)}(t) + c_n f_{n-2}^{(m)}(t) + d_n f_n^{(m)}(t) + g_n f_{n+2}^{(m)}(t),\\ = \xi_0 a_n\big[f_{n-1}^{(m)}(t) - f_{n+1}^{(m)}(t)\big]\\ + \xi a_n\big[f_{n-1}^{(m-1)}(t) - f_{n+1}^{(m-1)}(t)\big]\cos\omega t\end{aligned} \tag{13}$$

($m = 1,2,\ldots$) with the initial conditions at $t = -\infty$ given by

$$f_n^{(0)}(-\infty) = f_n^{(0)}, \quad f_n^{(m)}(-\infty) = 0 \ \ (m = 1,2,\ldots). \tag{14}$$

For $\xi = 0$, the system of dipoles is in equilibrium with Boltzmann distribution

$$W_0(\vartheta) = Z^{-1}e^{\sigma\cos^2\vartheta + \xi_0\cos\vartheta}, \tag{15}$$

where Z is the partition function (see Eq. (C5) in Appendix C), so that $f_n^{(0)} = \langle P_n\rangle_0$ can be calculated as

$$f_n^{(0)} = \int_0^\pi P_n(\cos\vartheta)W_0(\vartheta)\sin\vartheta\, d\vartheta. \tag{16}$$

Clearly, the equilibrium averages $f_n^{(0)}$ also satisfy the following five-term recurrence equation:

$$c_n f_{n-2}^{(0)} + d_n f_n^{(0)} + g_n f_{n+2}^{(0)} - \xi_0 a_n\big(f_{n-1}^{(0)} - f_{n+1}^{(0)}\big) = 0. \tag{17}$$

Equations (13) and (17) are seven-and five- term differential-recurrence relations, respectively, which can be solved for weak ac fields ($\xi \ll 1$) using matrix methods [32].

To proceed, we rearrange Eqs. (13) and (17) for $f_n^{(0)}$ and $f_n^{(m)}(t)$ ($m = 1,2,3,\ldots$) into matrix form as the set of the coupled linear matrix differential equations:

$$\frac{d}{dt}\mathbf{c}^{(1)}(t) + \mathbf{A}\mathbf{c}^{(1)}(t) = \xi(t)\mathbf{c}_1, \tag{18}$$

$$\frac{d}{dt}\mathbf{c}^{(m)}(t) + \mathbf{A}\mathbf{c}^{(m)}(t) = \xi(t)\mathbf{B}\mathbf{c}^{(m-1)}(t), \tag{19}$$

with the initial conditions $\mathbf{c}^{(0)}(-\infty) = \mathbf{c}^{(0)}$ and $\mathbf{c}^{(m)}(-\infty) = 0$ ($m = 1,2,3,\ldots$) yielded by Eq. (14). Here, $\xi(t) = \xi\cos\omega t$ and the infinite column vectors $\mathbf{c}^{(m)}(t)$ and $\mathbf{c}_1$ are given by

$$\mathbf{c}^{(m)}(t) = \begin{pmatrix} f_1^{(m)}(t)\\ f_2^{(m)}(t)\\ \vdots\\ f_n^{(m)}(t)\\ \vdots\end{pmatrix}, \quad \mathbf{c}_1 = \begin{pmatrix}\tau_D^{-1}a_1\\ 0\\ 0\\ \vdots\end{pmatrix} + \mathbf{B}\mathbf{c}^{(0)},$$

$$\mathbf{c}^{(0)} = \begin{pmatrix}\langle P_1\rangle_0\\ \langle P_2\rangle_0\\ \vdots\\ \langle P_n\rangle_0\\ \vdots\end{pmatrix},$$

while the matrix elements of the time-independent five-diagonal matrix $\mathbf{A}$ and two-diagonal matrix $\mathbf{B}$ are

$$\begin{aligned}(\mathbf{A})_{pq} &= \frac{1}{\tau_D}(\delta_{pq+2}c_p - \delta_{pq+1}\xi_0 a_p + \delta_{pq}d_p\\ &\quad + \delta_{pq-1}\xi_0 a_p + \delta_{pq-2}g_p),\\ (\mathbf{B})_{pq} &= \frac{1}{\tau_D}(\delta_{pq+1}a_p - \delta_{pq-1}a_p).\end{aligned}$$

Now, the column vector $\mathbf{c}^{(0)}$ can be evaluated via inversion of the system matrix $\mathbf{A}$ as (Ref. [16], Chap. 7)

$$\mathbf{c}^{(0)} = \mathbf{A}^{-1}\begin{pmatrix}\xi_0\tau_D^{-1}a_1\\ -\tau_D^{-1}c_2\\ 0\\ 0\\ \vdots\end{pmatrix}, \tag{20}$$

thereby yielding the initial condition vector $\mathbf{c}_1$ in Eq. (18) [we remark in passing that both Eqs. (20) and (16) yield identical results for $\langle P_n\rangle_0$]. Equations (18) and (19), which are coupled matrix first-order linear differential equations, may then be solved analytically, yielding

$$\mathbf{c}^{(1)}(t) = \int_{-\infty}^{t}\xi(t')e^{-\mathbf{A}(t-t')}\mathbf{c}_1 dt' = \xi\mathrm{Re}\big[\boldsymbol{\varphi}_1^{(1)}(\omega)e^{i\omega t}\big], \tag{21}$$

$$\begin{aligned}\mathbf{c}^{(2)}(t) &= \int_{-\infty}^{t}\xi(t')e^{-\mathbf{A}(t-t')}\mathbf{B}\int_{-\infty}^{t'}\xi(t'')e^{-\mathbf{A}(t'-t'')}\mathbf{c}_1 dt''dt'\\ &= \frac{\xi^2}{2}\mathrm{Re}\big[\boldsymbol{\varphi}_0^{(2)}(\omega) + \boldsymbol{\Phi}_2^{(2)}(2\omega)\boldsymbol{\varphi}_0^{(2)}(\omega)e^{2i\omega t}\big],\end{aligned} \tag{22}$$

$$\mathbf{c}^{(3)}(t) = \int_{-\infty}^{t} \xi(t')e^{-\mathbf{A}(t-t')}\mathbf{B}\int_{-\infty}^{t'} \xi(t'')e^{-\mathbf{A}(t'-t'')}\mathbf{B}\int_{-\infty}^{t''} \xi(t''')e^{-\mathbf{A}(t''-t''')}\mathbf{c}_1 dt''' dt'' dt'$$
$$= \frac{\xi^3}{4}\mathrm{Re}\left\{\left(2\mathrm{Re}\left[\boldsymbol{\Phi}_1^{(3)}(\omega)\right]\boldsymbol{\varphi}_0^{(2)}(\omega) + \boldsymbol{\Phi}_1^{(3)}(\omega)\boldsymbol{\Phi}_2^{(2)}(2\omega)\boldsymbol{\varphi}_0^{(2)}(\omega)\right)e^{i\omega t} + \boldsymbol{\Phi}_1^{(3)}(3\omega)\boldsymbol{\Phi}_2^{(2)}(2\omega)\boldsymbol{\varphi}_0^{(2)}(\omega)e^{3i\omega t}\right\}, \quad (23)$$

and so on to any desired order in m. Here the column vectors $\boldsymbol{\varphi}_1^{(1)}(\omega)$, $\boldsymbol{\varphi}_0^{(2)}(\omega)$ and matrixes $\boldsymbol{\Phi}_2^{(2)}(\omega)$, $\boldsymbol{\Phi}_1^{(3)}(\omega)$ are given by

$$\boldsymbol{\varphi}_1^{(1)}(\omega) = (\mathbf{A} + i\omega\mathbf{I})^{-1}\mathbf{c}_1, \quad (24)$$

$$\boldsymbol{\varphi}_0^{(2)}(\omega) = \mathbf{A}^{-1}\mathbf{B}(\mathbf{A} + i\omega\mathbf{I})^{-1}\mathbf{c}_1, \quad (25)$$

$$\boldsymbol{\Phi}_2^{(2)}(\omega) = (\mathbf{A} + i\omega\mathbf{I})^{-1}\mathbf{A}, \quad (26)$$

$$\boldsymbol{\Phi}_1^{(3)}(\omega) = (\mathbf{A} + i\omega\mathbf{I})^{-1}\mathbf{B}, \quad (27)$$

where $\mathbf{I}$ is the unit matrix, and we have used the fact that $e^{\mathbf{A}t}|_{t=-\infty} = 0$ (because all the eigenvalues λ_k of $\mathbf{A}$ are positive, i.e., $\lambda_k > 0$). We note that the column vectors $\boldsymbol{\varphi}_1^{(1)}(\omega)$ and $\boldsymbol{\varphi}_0^{(2)}(\omega)$ can also be written as

$$\boldsymbol{\varphi}_1^{(1)}(\omega) = \begin{pmatrix} \chi_{11}X_{11}(\omega) \\ \chi_{21}X_{21}(\omega) \\ \chi_{31}X_{31}(\omega) \\ \vdots \end{pmatrix}, \quad \boldsymbol{\varphi}_0^{(2)}(\omega) = \begin{pmatrix} \chi_{12}X_{10}^{(2)}(\omega) \\ \chi_{22}X_{20}^{(2)}(\omega) \\ \chi_{32}X_{30}^{(2)}(\omega) \\ \vdots \end{pmatrix}, \quad (28)$$

where $X_{n1}(\omega)$ and $X_{n0}^{(2)}(\omega)$ are the normalized [i.e., $X_{n1}(0) = X_{n0}^{(2)}(0) = 1$] linear and second-order nonlinear dc dynamic susceptibilities, respectively, while $\chi_{n1} = [\boldsymbol{\varphi}_1^{(1)}(0)]_n$ and $\chi_{m2} = [\boldsymbol{\Phi}_1^{(3)}(0)\boldsymbol{\varphi}_0^{(2)}(0)]_m$ are the corresponding static susceptibilities (they are evaluated in Appendix A).

These matrix solutions [Eqs. (21), (22), and (23)] are very useful for computational purposes. As far as the practical calculation is concerned, we approximate all infinite matrices and column vectors involved by the corresponding matrices and column vectors of finite dimensions $N\times N$ and N, respectively. The value of N, depending on the numerical values of the model parameters (ξ_0,σ) as well as on the rank n and the order of perturbation solution m of $f_n^{(m)}(t)$ required, must be chosen according to the desired degree of accuracy. For example, in evaluation of $f_1^{(m)}(t)$ and $f_2^{(m)}(t)$ for $m = 1,2,3$, and for σ and ξ_0 up to 20, the matrix dimension N need not exceed 60 for an accuracy of not less than 6 significant digits in most instances. The numerical results obtained using this method are in complete agreement with those from the independent numerical methods developed in Refs. [16,22,23].

IV. TWO-MODE APPROXIMATION FOR LINEAR RESPONSE

Although the matrix solutions obtained in the previous section allow us to evaluate nonlinear responses numerically, it does not give us a qualitative understanding of the relaxation dynamics of the system. However, such a qualitative understanding of the dynamical behavior is provided by the two-mode approximation, which is based on the large separation of the timescales of the fast intrawell and slow overbarrier (interwell) relaxation processes in the double-well mean-field potential, Eq. (4) [16,26] (see also Appendix B). In this section, we shall now show how the two-mode approximation explains the relaxation dynamics in the presence of a weak ac field ($\xi \ll 1$), yielding a simple analytic description of the linear response characteristics of dipolar particles in the potential Eq. (4) for all ranges of the model parameters σ and ξ_0. According to Eq. (12), the ac stationary linear response is governed by the response functions $f_n^{(1)}(t) = [\mathbf{c}^{(1)}(t)]_n$, which are given by the nth element of the column vector $\mathbf{c}^{(1)}(t)$ in Eq. (21), so that

$$f_n^{(1)}(t) = \xi\mathrm{Re}\left\{\left[\boldsymbol{\varphi}_1^{(1)}(\omega)\right]_n e^{i\omega t}\right\} = \xi\mathrm{Re}\left[F_n^{(1)}(\omega)e^{i\omega t}\right], \quad (29)$$

where $F_n^{(1)}(\omega) = \chi_{n1}X_{n1}(\omega)$, and $X_{n1}(\omega)$ and $\chi_{n1} = [\boldsymbol{\varphi}_1^{(1)}(0)]_n$ are the normalized linear dynamic and static susceptibilities, respectively, and are defined by Eq. (28). The static susceptibilities χ_{n1} are expressed via the expectation values of the Legendre polynomials at equilibrium as (see Appendix A)

$$\chi_{n1} = \langle P_n P_1\rangle_0 - \langle P_n\rangle_0\langle P_1\rangle_0. \quad (30)$$

According to linear response theory, the normalized dynamic susceptibility $X_{n1}(\omega)$ is defined by the Kubo equation [33,34],

$$X_{n1}(\omega) = 1 - i\omega\int_0^\infty e^{-i\omega t}\Phi_{n1}(t)dt, \quad (31)$$

where $\Phi_{n1}(t)$ is the normalized equilibrium correlation function viz.

$$\Phi_{n1}(t) = \frac{\langle P_n[\cos\vartheta(0)]P_1[\cos\vartheta(t)]\rangle_0 - \langle P_n\rangle_0\langle P_1\rangle_0}{\langle P_n P_1\rangle_0 - \langle P_n\rangle_0\langle P_1\rangle_0}, \quad (32)$$

which comprises, in general, an infinity of relaxation modes (decaying exponentials), i.e., [16,33]

$$\Phi_{n1}(t) = \sum_{k=1}^{\infty} c_k^n e^{-\lambda_k t}. \quad (33)$$

Here $\lambda_1,\lambda_2,\lambda_3,\ldots$ are the eigenvalues of the system matrix $\mathbf{A}$ and, therefore, the eigenvalues of the Fokker-Planck operator L_{FP} defined by Eq. (3). These eigenvalues can be evaluated from the characteristic equation [16]

$$\det(\lambda\mathbf{I} - \mathbf{A}) = 0. \quad (34)$$

For high potential barriers, $\Delta V = \sigma(1 - \xi_0/2\sigma)^2 \gg 1$, the relaxation process is dominated by the smallest nonvanishing eigenvalue λ_1, which is much smaller than all other eigenvalues, i.e., $\lambda_1 \ll \lambda_2,\lambda_3,\ldots$ [16]. This eigenvalue has an Arrhenius-like behavior, $\lambda_1 \sim e^{-\Delta V}$, and is associated with the slowest overbarrier relaxation mode (the explicit equations for λ_1 in the low- and high-barrier limits are given by Eqs. (C6) and (C9) in Appendix C, respectively). All other eigenvalues $\lambda_2,\lambda_3,\ldots$ are associated with the fast "intrawell" relaxation modes and weakly depend on temperature [16,26]. Thus, one

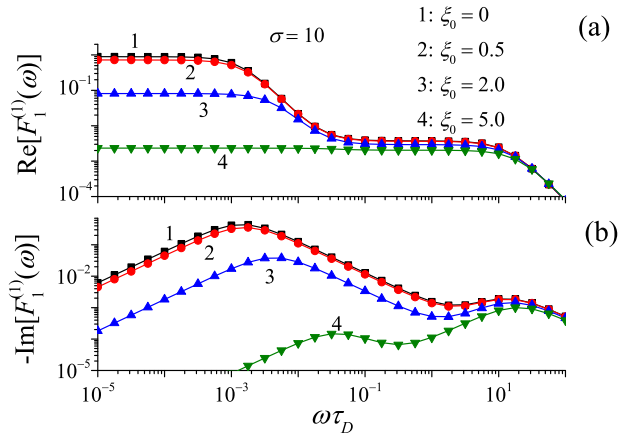

FIG. 1. Real (a) and imaginary (b) parts of the linear susceptibility $F_1^{(1)}(\omega) = \chi_{11}X_{11}(\omega)$ vs. the normalized frequency $\omega\tau_D$ for various dc field amplitudes ξ_0 with the anisotropy parameter $\sigma = 10$. Solid lines: the matrix solution, Eq. (21). Symbols: the two-mode approximation Eq. (36) with parameters calculated from Eqs. (34), (B7), (B8), (B11), and (B12).

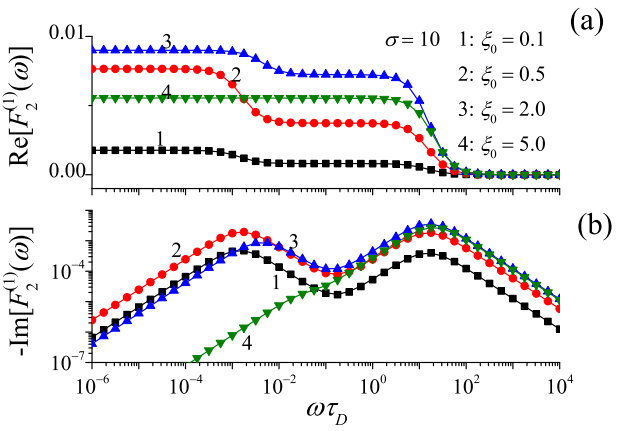

FIG. 2. Real (a) and imaginary (b) parts of the linear Kerr effect response $F_2^{(1)}(\omega) = \chi_{21}X_{21}(\omega)$ vs. $\omega\tau_D$ for various dc field amplitudes ξ_0 with the anisotropy parameter $\sigma = 10$. Solid lines: the matrix solution, Eq. (21). Symbols: the two-mode approximation Eq. (36) with the parameters calculated from Eqs. (34), (B7), (B8), (B11), and (B12).

may suppose [16,26,27] that $\Phi_{n1}(t)$ may be approximated by two relaxation modes only,

$$\Phi_{n1}(t) \approx \Delta_{n1}e^{-\lambda_1 t} + (1-\Delta_{n1})e^{-t/\tau_W^{(n1)}}, \tag{35}$$

where $\tau_W^{(n1)}$ is the inverse of the characteristic frequency of the near degenerate high-frequency modes while Δ_{n1} and $1-\Delta_{n1}$ are amplitudes accounting for the overbarrier and intrawell relaxation processes, respectively. The parameters Δ_{n1} and $\tau_W^{(n1)}$ can be expressed in terms of the characteristic relaxation times of the correlation function $\Phi_{n1}(t)$ [16,27] (details in Appendices B and C). By inserting Eq. (35) into Eq. (31), the normalized dynamic susceptibility $X_{n1}(\omega)$ can be obtained analytically as the sum of two Lorentzians, viz.,

$$X_{n1}(\omega) \approx \frac{\Delta_{n1}}{1+i\omega/\lambda_1} + \frac{1-\Delta_{n1}}{1+i\omega\tau_W^{(n1)}}. \tag{36}$$

In particular, both for the linear dielectric and Kerr-effect response, the parameters Δ_{n1} and $\tau_W^{(n1)}$ in Eq. (36) are evaluated by letting $n = 1$ and $n = 2$ in Eqs. (B11) and (B12) of Appendices B, respectively.

In Figs. 1 and 2, we show the real and imaginary parts of $X_{11}(\omega)$ and $X_{12}(\omega)$ calculated using the matrix solution, Eqs. (21) and (24), and the approximate Eq. (36). These figures indicate that there is no practical difference between the matrix solution and the two-mode approximation (the maximum relative deviation between the corresponding curves does not exceed a few percent). Clearly, two peaks appear in the spectra of the imaginary parts $-\mathrm{Im}[X_{11}(\omega)]$ and $-\mathrm{Im}[X_{21}(\omega)]$ and two dispersion bands are noticeable in the spectra of the real parts $\mathrm{Re}[X_{11}(\omega)]$ and $\mathrm{Re}[X_{21}(\omega)]$. The low-frequency part of the spectra is dominated by the slowest overbarrier relaxation mode. The characteristic frequency $\omega_{\max}$ and the half-width $\Delta\omega$ of this band are determined by smallest nonvanishing eigenvalue λ_1. The eigenvalue λ_1 is related to the frequency $\omega_{\max}$ of the low-frequency peak in the spectra $-\mathrm{Im}[X_{11}(\omega)]$ and $-\mathrm{Im}[X_{21}(\omega)]$, where they attain maxima, and/or the half-width $\Delta\omega$ of the spectra of the real part of the susceptibility $\mathrm{Re}[X_{11}(\omega)]$ and $\mathrm{Re}[X_{21}(\omega)]$ via

$$\lambda_1 \approx \omega_{\max} \approx \Delta\omega. \tag{37}$$

Here, comparison of λ_1 as extracted from the spectra $X_{11}(\omega)$ and $X_{12}(\omega)$ via Eq. (37) with λ_1 calculated independently via the system matrix $\mathbf{A}$ shows that both methods yield identical results. Our calculations indicate that on increasing the dc field parameter ξ_0, the magnitude of the low-frequency band drastically decreases due to the depletion of the population in the shallower potential well of the potential V [16,26], which results in the virtual disappearance of the low-frequency peak in the spectra $-\mathrm{Im}[X_{11}(\omega)]$ and $-\mathrm{Im}[X_{21}(\omega)]$ (see Figs. 1 and 2). Furthermore, the low-frequency peak shifts monotonically to higher frequencies with increasing ξ_0. The high-frequency peaks of $-\mathrm{Im}[X_{11}(\omega)]$ and $-\mathrm{Im}[X_{21}(\omega)]$ are due to the near-degenerate high-frequency intrawell modes corresponding to the eigenvalues λ_k ($k \geqslant 2$). These individual intrawell modes are indistinguishable in the spectra of $-\mathrm{Im}[X_{11}(\omega)]$ and $-\mathrm{Im}[X_{21}(\omega)]$ appearing merely as a single high-frequency Lorentzian band (see Figs. 1 and 2).

Now we shall show that the two-mode approximation yields also an accurate description of the dynamic Kerr-effect spectra and nonlinear dielectric relaxation.

V. TWO-MODE APPROXIMATION FOR DYNAMIC KERR EFFECT

The second-rank response $f_2^{(2)}(t) = [\mathbf{c}^{(2)}(t)]_2$ governing the dynamic Kerr-effect response can be written as a sum of a dc term and a term depending on $e^{2i\omega t}$, so that

$$f_2^{(2)}(t) = \xi^2 \mathrm{Re}\left[F_{2,0}^{(2)}(\omega) + F_{2,2}^{(2)}(\omega)e^{2i\omega t}\right], \tag{38}$$

where $F_{2,0}^{(2)}(\omega) = [\boldsymbol{\varphi}_0^{(2)}(\omega)]_2/2$ and $F_{2,2}^{(2)}(\omega) = [\boldsymbol{\Phi}_2^{(2)}(2\omega)\boldsymbol{\varphi}_0^{(2)}(\omega)]_2/2$. In the two-mode approximation,

the Fourier amplitudes $F^{(2)}_{2,0}(\omega)$ and $F^{(2)}_{2,2}(\omega)$ can be written as

$$F^{(2)}_{2,0}(\omega) \approx \frac{\chi_{22}}{2} X^{(2)}_{20}(\omega), \tag{39}$$

$$F^{(2)}_{2,2}(\omega) \approx \frac{\chi_{22}}{2} X_{22}(2\omega) X'^{(2)}_{20}(\omega), \tag{40}$$

where the static susceptibility χ_{22} is given by (see Appendix A)

$$\chi_{22} = \frac{1}{3}\left(\langle P_2^2\rangle_0 - \langle P_2\rangle_0^2\right) - \langle P_1\rangle_0(\langle P_1 P_2\rangle_0 - \langle P_1\rangle_0\langle P_2\rangle_0), \tag{41}$$

and the dynamic susceptibilities $X^{(2)}_{20}(\omega)$, $X'^{(2)}_{20}(\omega)$, and $X_{22}(\omega)$ may again be written in the two-mode approximation as

$$X^{(2)}_{20}(\omega) \approx \frac{\Delta_{20}}{1+i\omega/\lambda_1} + \frac{1-\Delta_{20}}{1+i\omega\tau_W^{(20)}}, \tag{42}$$

$$X'^{(2)}_{20}(\omega) \approx \frac{\Delta'_{20}}{1+i\omega/\lambda_1} + \frac{1-\Delta'_{20}}{1+i\omega\tau_W^{(\prime 20)}}, \tag{43}$$

$$X_{22}(\omega) \approx \frac{\Delta_{22}}{1+i\omega\tau_{22}} + \frac{1-\Delta_{22}}{1+i\omega\tau_W^{(22)}}. \tag{44}$$

In the Kerr effect response, Δ_{20} and $\tau_W^{(20)}$ in Eq. (42) can be calculated [24] via Eqs. (B11) and (B12), where the time constants τ_{20} and $\tau_{20}^{\rm eff}$ are estimated from the low- and high-frequency asymptotes, Eq. (B6), yielding

$$\tau_{20} = -\lim_{\omega\to 0}\frac{1}{\omega}\mathrm{Im}\left\{\frac{1}{\chi_{22}}\left[\boldsymbol{\varphi}^{(2)}_0(\omega)\right]_2\right\} \text{ and}$$

$$\tau_{20}^{\rm eff} = \lim_{\omega\to\infty}\frac{1}{\omega}\mathrm{Im}\left\{\frac{\chi_{22}}{\left[\boldsymbol{\varphi}^{(2)}_0(\omega)\right]_2}\right\}.$$

However, analytic equations for the other parameters, Δ'_{20}, $\tau_W^{\prime(20)}$, Δ_{22}, τ_{22}, and $\tau_W^{(22)}$, like Eqs. (B7) and (B8) no longer exist. Therefore, they are treated as adjustable parameters.

The spectra of the dc component of the second-order Kerr-effect $\mathrm{Re}[F^{(2)}_{2,0}(\omega)]$ and the Kerr-effect second harmonic component $\mathrm{Re}[F^{(2)}_{2,2}(\omega)]$ are shown in Fig. 3 for various dc field parameters ξ_0 as calculated from the matrix and two-mode approximation solutions. Just as with the linear response, no practical difference exists between the matrix and two-mode approximation solutions.

VI. HIGHER-ORDER DIELECTRIC AND KERR-EFFECT RESPONSES

In the nonlinear dielectric response, where the terms of order ξ^2 and ξ^3 cannot be neglected, the second-rank response function $f^{(2)}_1(t) = [\mathbf{c}^{(2)}(t)]_1$, which is proportional to ξ^2, can be written, by inspection of Eq. (22), as a sum of a dc term and a term depending on $e^{2i\omega t}$ so that

$$f^{(2)}_1(t) = \xi^2\mathrm{Re}\left[F^{(2)}_{1,0}(\omega) + F^{(2)}_{1,2}(\omega)e^{2i\omega t}\right], \tag{45}$$

where

$$F^{(2)}_{1,0}(\omega) = \frac{1}{2}\left[\boldsymbol{\varphi}^{(2)}_0(\omega)\right]_1 \text{ and } F^{(2)}_{1,2}(\omega) = \frac{1}{2}\left[\boldsymbol{\Phi}^{(2)}_2(2\omega)\boldsymbol{\varphi}^{(2)}_0(\omega)\right]_1.$$

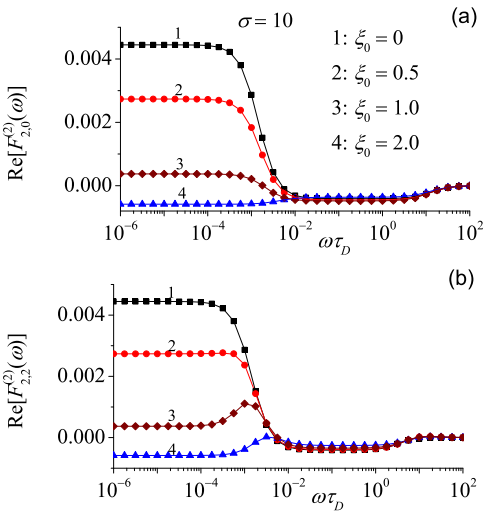

FIG. 3. Dc component of the second-order Kerr-effect $\mathrm{Re}[F^{(2)}_{2,0}(\omega)]$ (a) and the Kerr-effect second harmonic component $\mathrm{Re}[F^{(2)}_{2,2}(\omega)]$ (b) vs. $\omega\tau_D$ for various dc field amplitudes ξ_0 with the anisotropy parameter $\sigma = 10$. Solid lines: the matrix solution. Symbols: the two-mode approximation Eqs. (39) and (40) using fitting parameters.

Furthermore, the third-order contribution $f^{(3)}_1(t) = [\mathbf{c}^{(3)}(t)]_1$, which is proportional to ξ^3, can be written as

$$f^{(3)}_1(t) = \xi^3\mathrm{Re}\left[F^{(3)}_{1,1}(\omega)e^{i\omega t} + F^{(3)}_{1,3}(\omega)e^{3i\omega t}\right], \tag{46}$$

where

$$F^{(3)}_{1,1}(\omega) = \tfrac{1}{4}\left\{2\left[\mathrm{Re}\left[\boldsymbol{\Phi}^{(3)}_1(\omega)\right]\boldsymbol{\varphi}^{(2)}_0(\omega)\right]_1 + \left[\boldsymbol{\Phi}^{(3)}_1(\omega)\boldsymbol{\Phi}^{(2)}_2(2\omega)\boldsymbol{\varphi}^{(2)}_0(\omega)\right]_1\right\}$$

and

$$F^{(3)}_{1,3}(\omega) = \tfrac{1}{4}\left[\boldsymbol{\Phi}^{(3)}_1(3\omega)\boldsymbol{\Phi}^{(2)}_2(2\omega)\boldsymbol{\varphi}^{(2)}_0(\omega)\right]_1.$$

In the two-mode approximation, the Fourier amplitudes $F^{(2)}_{1,0}(\omega)$, $F^{(2)}_{1,2}(\omega)$, $F^{(3)}_{1,1}(\omega)$, and $F^{(3)}_{1,3}(\omega)$ can be written as

$$F^{(2)}_{1,0}(\omega) \approx \frac{\chi_{12}}{2} X^{(2)}_{10}(\omega), \tag{47}$$

$$F^{(2)}_{1,2}(\omega) \approx \frac{\chi_{12}}{2} X_{12}(2\omega) X'^{(2)}_{10}(\omega), \tag{48}$$

$$F^{(3)}_{1,1}(\omega) \approx \frac{\chi_{13}}{4}\left\{2\mathrm{Re}[X_{13}(\omega)]X'^{(2)}_{10}(\omega) + X_{13}(\omega)X_{12}(2\omega)X'^{(2)}_{10}(\omega)\right\}, \tag{49}$$

$$F^{(3)}_{1,3}(\omega) \approx \frac{\chi_{13}}{4} X_{13}(3\omega)X_{12}(2\omega)X'^{(2)}_{10}(\omega), \tag{50}$$

where the generalized dynamic susceptibilities $X^{(2)}_{10}(\omega)$, $X'^{(2)}_{10}(\omega)$, $X_{12}(\omega)$, and $X_{13}(\omega)$ are given by

$$X^{(2)}_{10}(\omega) \approx \frac{\Delta_{10}}{1+i\omega/\lambda_1} + \frac{1-\Delta_{10}}{1+i\omega\tau_W^{(10)}}, \tag{51}$$

$$X'^{(2)}_{10}(\omega) \approx \frac{\Delta'_{10}}{1+i\omega/\lambda_1} + \frac{1-\Delta'_{10}}{1+i\omega\tau_W^{(\prime 10)}}, \tag{52}$$

$$X_{12}(\omega) \approx \frac{\Delta_{12}}{1+i\omega\tau_{12}} + \frac{1-\Delta_{12}}{1+i\omega\tau_W^{(12)}}, \tag{53}$$

$$X_{13}(\omega) \approx \frac{\Delta_{13}}{1+i\omega/\lambda_1} + \frac{1-\Delta_{13}}{1+i\omega\tau_W^{(13)}}, \tag{54}$$

and the static susceptibilities χ_{12} and χ_{13} are (see Appendix A)

$$\chi_{12} = \tfrac{1}{3}\big(\langle P_2 P_1\rangle_0 - \langle P_2\rangle_0\langle P_1\rangle_0\big) - \langle P_1\rangle_0\big(\langle P_1^2\rangle_0 - \langle P_1\rangle_0^2\big), \tag{55}$$

$$\begin{aligned}\chi_{13} = {} & \tfrac{1}{6}\big(\langle P_1^4\rangle_0 - \langle P_1^3\rangle_0\langle P_1\rangle_0\big) - \tfrac{1}{2}\langle P_1^2\rangle_0\big(\langle P_1^2\rangle_0 - \langle P_1\rangle_0^2\big) \\ & + \langle P_1\rangle_0^2\big(\langle P_1^2\rangle_0 - \langle P_1\rangle_0^2\big) - \tfrac{1}{2}\langle P_1\rangle_0\big(\langle P_1^3\rangle_0 - \langle P_1\rangle_0\langle P_1^2\rangle_0\big).\end{aligned} \tag{56}$$

Similarly, the third-order contribution $f_2^{(3)}(t) = [\mathbf{c}^{(3)}(t)]_2$ to the second-rank response function $f_2(t)$ governing the Kerr-effect relaxation is

$$f_2^{(3)}(t) = \xi^3 \mathrm{Re}\big[F_{2,1}^{(3)}(\omega)e^{i\omega t} + F_{2,3}^{(3)}(\omega)e^{3i\omega t}\big], \tag{57}$$

where

$$\begin{aligned}F_{2,1}^{(3)}(\omega) = {} & \tfrac{1}{2}\big[\mathrm{Re}\big[\boldsymbol{\Phi}_1^{(3)}(\omega)\big]\boldsymbol{\varphi}_0^{(2)}(\omega) \\ & + \tfrac{1}{2}\boldsymbol{\Phi}_1^{(3)}(\omega)\boldsymbol{\Phi}_2^{(2)}(2\omega)\boldsymbol{\varphi}_0^{(2)}(\omega)\big]_2,\end{aligned}$$

and

$$F_{2,3}^{(3)}(\omega) = \tfrac{1}{4}\big[\boldsymbol{\Phi}_1^{(3)}(3\omega)\boldsymbol{\Phi}_2^{(2)}(2\omega)\boldsymbol{\varphi}_0^{(2)}(\omega)\big]_2.$$

Again, using the two-mode approximation, these Fourier amplitudes are

$$\begin{aligned}F_{2,1}^{(3)}(\omega) \approx {} & \frac{\chi_{23}}{4}\big\{2\mathrm{Re}[X_{23}(\omega)]X_{20}'^{(2)}(\omega) \\ & + X_{23}(\omega)X_{22}(2\omega)X_{20}'^{(2)}(\omega)\big\},\end{aligned} \tag{58}$$

$$F_{2,3}^{(3)}(\omega) \approx \frac{\chi_{23}}{4}X_{23}(3\omega)X_{22}(2\omega)X_{20}'^{(2)}(\omega), \tag{59}$$

where the dynamic susceptibility $X_{23}(\omega)$ is given by

$$X_{23}(\omega) \approx \frac{\Delta_{23}}{1+i\omega/\lambda_1} + \frac{1-\Delta_{23}}{1+i\omega\tau_W^{(23)}}, \tag{60}$$

and the static susceptibility χ_{23} is (see Appendix A)

$$\begin{aligned}\chi_{23} = {} & \tfrac{1}{6}\big(\langle P_1^3 P_2\rangle_0 - \langle P_1^3\rangle_0\langle P_2\rangle_0\big) - \tfrac{1}{2}\langle P_1 P_2\rangle_0\big(\langle P_1^2\rangle_0 - \langle P_1\rangle_0^2\big) \\ & + \langle P_1\rangle_0\langle P_2\rangle_0\big(\langle P_1^2\rangle_0 - \langle P_1\rangle_0^2\big) \\ & - \tfrac{1}{2}\langle P_1\rangle_0\big(\langle P_1^2 P_2\rangle_0 - \langle P_1\rangle_0\langle P_1 P_2\rangle_0\big).\end{aligned} \tag{61}$$

The spectra of the dc component of the second-order nonlinear dielectric response $\mathrm{Re}[F_{1,0}^{(2)}(\omega)]$, the second harmonic component of the second-order nonlinear dielectric response $\mathrm{Re}[F_{1,2}^{(2)}(\omega)]$, the fundamental component of the third-order nonlinear dielectric response $\mathrm{Re}[F_{1,1}^{(3)}(\omega)]$, the 3rd harmonic component of the third-order nonlinear dielectric response $\mathrm{Re}[F_{1,3}^{(3)}(\omega)]$, the fundamental component of the third-order nonlinear Kerr-effect response $\mathrm{Re}[F_{2,1}^{(3)}(\omega)]$, and the third harmonic component of the third-order nonlinear Kerr-effect response $\mathrm{Re}[F_{2,3}^{(3)}(\omega)]$ are shown in Figs. 4 and 5 for various dc field parameters ξ_0, which are calculated using the matrix and two-mode approximation solutions. Just as with the other responses, the matrix and two-mode approximation solutions are in complete agreement.

For the particular case of zero anisotropy $\sigma = 0$ and zero dc bias field $\xi_0 = 0$, the equations we have obtained above for the dielectric and Kerr-effect response functions $f_1(t)$ and $f_2(t)$ subjected to combined ac and dc fields reduce to the known results [5], namely,

$$\begin{aligned}f_1(t) = {} & \frac{\xi}{3}\frac{\cos\omega t + \omega\tau_D \sin\omega t}{1+\omega^2\tau_D{}^2} - \frac{\xi^3}{45}\Bigg[\frac{\big(27-13\tau_D{}^2\omega^2\big)\cos\omega t}{4\big(1+\tau_D{}^2\omega^2\big)^2\big(9+4\tau_D{}^2\omega^2\big)} + \frac{\omega\tau_D\big(21+\tau_D{}^2\omega^2\big)\sin\omega t}{2\big(1+\tau_D{}^2\omega^2\big)^2\big(9+4\tau_D{}^2\omega^2\big)} \\ & + 3\frac{\big(3-17\tau_D{}^2\omega^2\big)\cos 3\omega t + 2\omega\tau_D\big(3\tau_D{}^2\omega^2-7\big)\sin 3\omega t}{4\big(9+4\tau_D{}^2\omega^2\big)\big(1+\tau_D{}^2\omega^2\big)\big(1+9\tau_D{}^2\omega^2\big)}\Bigg] + o(\xi^3),\end{aligned} \tag{62}$$

$$f_2(t) = \frac{\xi^2}{30\big(1+\omega^2\tau_D{}^2\big)}\left[1 + \frac{\big(3-2\omega^2\tau_D{}^2\big)\cos 2\omega t + 5\omega\tau_D\sin 2\omega t}{3\big(1+4\omega^2\tau_D{}^2/9\big)}\right]. \tag{63}$$

VII. DC COMPONENTS OF THE DIELECTRIC AND KERR-EFFECT AC STATIONARY RESPONSES

Now we consider in detail the *time-independent but frequency-dependent* components of the dielectric and Kerr-effect ac stationary responses $\overline{f_1}(\omega)$ and $\overline{f_2}(\omega)$, defined as the time averages over a period of the ac field:

$$\begin{aligned}\overline{f_n}(\omega) = {} & \frac{\omega}{2\pi}\int_0^{2\pi/\omega} f_n(t)\,dt = \langle P_n\rangle_0 + \xi^2\mathrm{Re}\big[F_{n,0}^{(2)}(\omega)\big] \\ & + o(\xi^2), \quad (n=1,2).\end{aligned} \tag{64}$$

First, in contrast to the Kerr-effect response, the dc component of the dielectric response $\overline{f_1}(\omega)$ is nonzero only when an external dc bias field is superimposed on the ac field. The nonlinear ac field contributions to $\overline{f_1}(\omega)$ and $\overline{f_2}(\omega)$ are of order ξ^2 and both strongly depend on the dc bias field ξ_0 and the anisotropy parameter σ. According to the results of Sec. VI, in the two-mode approximation, both $\overline{f_1}(\omega)$ and $\overline{f_2}(\omega)$ may be approximated by a sum of two Lorentzians, viz.,

$$\overline{f_n}(\omega) \approx \langle P_n\rangle_0 + \frac{\chi_{n2}\xi^2}{2}\left(\frac{\Delta_{n0}}{1+(\omega/\lambda_1)^2} + \frac{1-\Delta_{n0}}{1+\big(\omega\tau_W^{(n0)}\big)^2}\right), \quad (n=1,2), \tag{65}$$

where χ_{12} and χ_{22} are given by Eqs. (55) and (41), respectively.

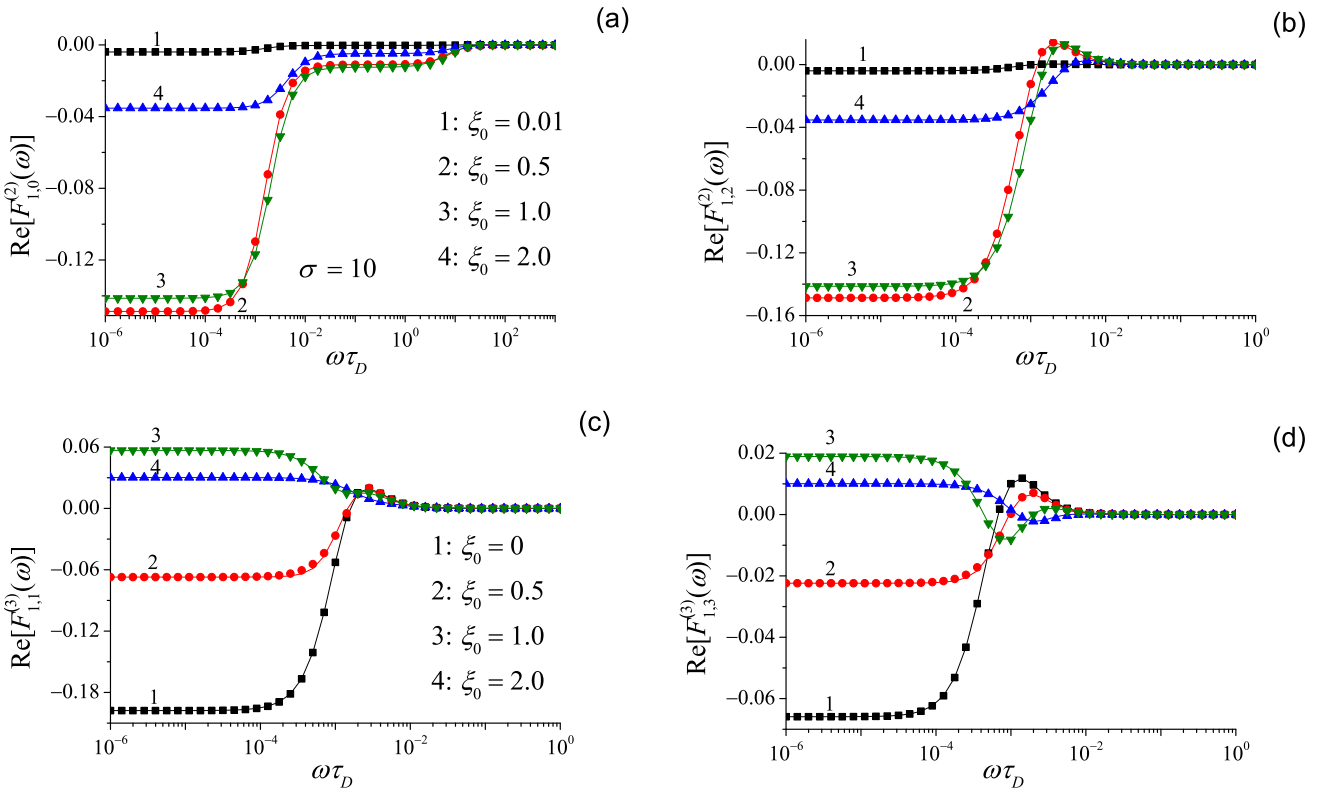

FIG. 4. Dc component $\mathrm{Re}[F^{(2)}_{1,0}(\omega)]$ (a), the second harmonic component $\mathrm{Re}[F^{(2)}_{1,2}(\omega)]$ (b), the fundamental component $\mathrm{Re}[F^{(3)}_{1,1}(\omega)]$ (c), and the third harmonic component $\mathrm{Re}[F^{(3)}_{1,3}(\omega)]$ (d) of the nonlinear dielectric response vs. $\omega\tau_D$ for various dc field amplitudes ξ_0 with $\sigma = 10$. Solid lines: the matrix solution. Symbols: the two-mode approximation Eqs. (47), (48), (49), and (50) using fitting parameters.

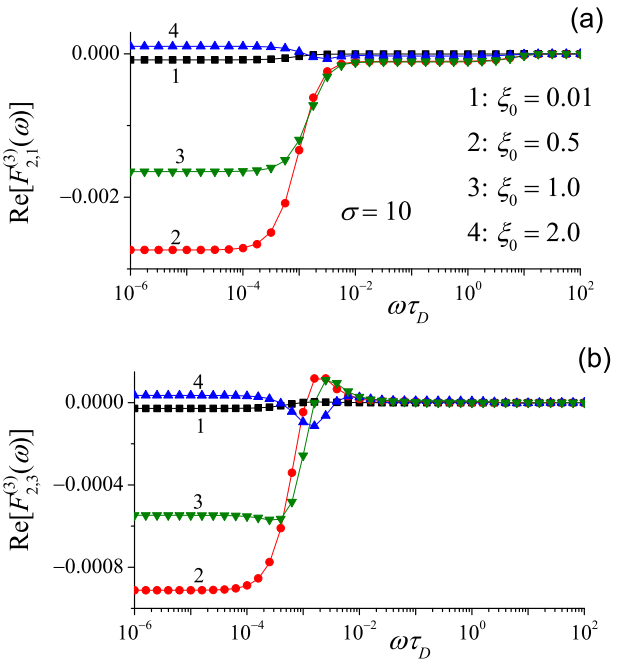

FIG. 5. Fundamental component $\mathrm{Re}[F^{(3)}_{2,1}(\omega)]$ (a) and the third harmonic component $\mathrm{Re}[F^{(3)}_{2,3}(\omega)]$ (b) of the third-order Kerr effect vs. $\omega\tau_D$ for various dc field amplitudes ξ_0 with the anisotropy parameter $\sigma = 10$. Solid lines: the matrix solution. Symbols: the two-mode approximation Eqs. (58) and (59) using fitting parameters.

In Fig. 6, we plot $\overline{f_1}(\omega)$ and $\overline{f_2}(\omega)$ as functions of frequency in order to illustrate the nonlinear effects induced by the ac field in the dc components $\overline{f_1}(\omega)$ and $\overline{f_2}(\omega)$, which exhibit a pronounced frequency dependence. Clearly, the approximate Eq. (65) and is in agreement with the numerical calculations. By inspection of Fig. 6, two distinct low- and high-frequency dispersion regions appear in the spectra of $\overline{f_1}(\omega)$ and $\overline{f_2}(\omega)$, just as with the real part of the dynamic susceptibilities $\mathrm{Re}[X_{11}(\omega)]$ (cf. Fig. 1). The low-frequency dispersion region of each of the two functions $\overline{f_1}(\omega)$ and $\overline{f_2}(\omega)$ is clearly governed by the barrier-crossing relaxation modes with the *same* characteristic frequency $\omega_1 = \lambda_1$, *indicating that the overbarrier relaxation time may be determined directly from measurements of the dc responses* $\overline{f_1}(\omega)$ and $\overline{f_2}(\omega)$. In addition, for weak ac fields, the characteristic frequency ω_1 of this low-frequency band is associated with the overbarrier relaxation processes and may be determined as $\omega_1 = \lambda_1$. Now, at the opposite end of the spectrum, the high-frequency band is due to "intrawell" relaxation modes. These individual near-degenerate high-frequency modes are, however, virtually indistinguishable in the frequency spectra of $\overline{f_1}(\omega)$ and $\overline{f_2}(\omega)$, appearing merely as a single high-frequency relaxation band, just as with $\mathrm{Re}[X_{11}(\omega)]$ (see Fig. 1). The results clearly demonstrate that the dc components of the ac stationary nonlinear dielectric and Kerr-effect responses contain the same information about the relaxation processes as the linear and nonlinear dynamic susceptibilities. This fact suggests that a new method of measurement of the overbarrier relaxation time are possible

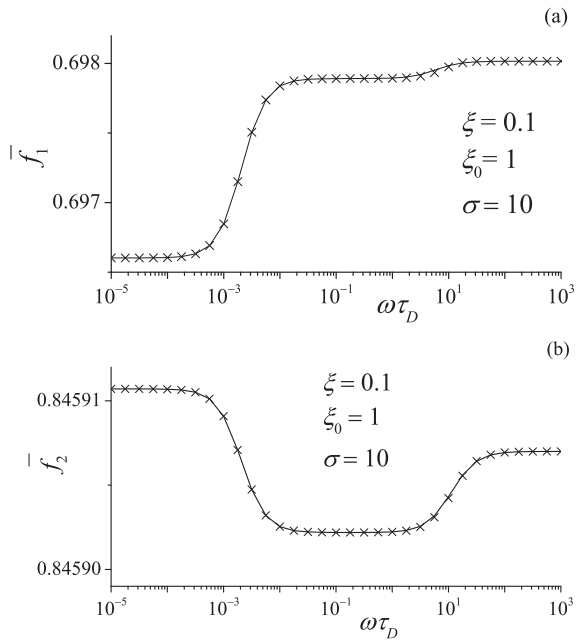

FIG. 6. dc components $\overline{f_1}(\omega)$ (a) and $\overline{f_2}(\omega)$ (b) vs. $\omega\,\tau_D$ with $\sigma = 10, \xi = 0.1$, and $\xi_0 = 1$ showing pronounced frequency-dependence, including two distinct dispersion regions caused by the entanglement of the dc and ac responses. Solid lines: the matrix solution. Crosses: the two-mode approximation Eq. (65).

via the dc component of dielectric (or magnetic) relaxation and birefringence.

VIII. GENERALIZATION TO ANOMALOUS RELAXATION

Now, one of the most noteworthy features of the dielectric relaxation of disordered materials and complex liquids such as glass-forming liquids, liquid crystals, amorphous polymers, etc., is the failure of the Debye theory [1] of normal dielectric relaxation to adequately describe the low-frequency spectra of their linear dielectric susceptibilities. The relaxation processes in such complex systems are characterized by the temporally nonlocal behavior arising from the energetic disorder, which produces obstacles or traps, simultaneously delaying the motion of the particle and producing memory effects. A significant amount of experimental data on anomalous relaxation of complex liquids supports an empirical equation of Havriliak-Negami [35]:

$$\chi_{\rm HN}(\omega) = \frac{\chi_S}{[1 + (i\omega\,\tau_D)^{\alpha}]^{\nu}}, \tag{66}$$

where χ_S is the static susceptibility and α $(0 < \alpha \leqslant 1)$ and ν $(0 < \nu \leqslant 1)$ are parameters with values, which are usually obtained by fitting to experimental data. For the particular cases $\nu = 1$ and $\alpha = 1$, Eq. (66) reduces, respectively, to other well-known phenomenological equations of Cole and Cole [36] and Cole and Davidson [37]:

$$\chi_{CC}(\omega) = \frac{\chi_S}{1 + (i\omega\,\tau_D)^{\alpha}}, \tag{67}$$

$$\chi_{CD}(\omega) = \frac{\chi_S}{(1 + i\omega\,\tau_D)^{\nu}}. \tag{68}$$

In the context of the linear susceptibility, Eqs. (66)–(68), the Cole-Cole parameter α is a *broadening* parameter because the dielectric loss spectrum broadens as α is reduced while the Cole-Davidson parameter ν in Eqs. (66) and (68) is a *skewing* parameter. The interested reader can find detailed discussions of anomalous relaxation behavior in complex disordered systems and various underlying microscopic models in Refs. [16] and [38–48]. Equations (66)–(68), which are generalizations of the Debye equation for the complex susceptibility, viz.,

$$\chi_D(\omega) = \frac{\chi_S}{1 + i\omega\tau_D}, \tag{69}$$

may be derived using a variety of microscopic models of the relaxation process. For example, Debye [1] extended Einstein's treatment of the translational Brownian motion to the rotational Brownian motion of noninteracting permanent dipoles subjected to an external time-varying field. It might also happen that the motion that prevails is different for different kinds of dipoles. Moreover, both large- and small-jump transitions may exist simultaneously. The above observations lead us to the second microscopic (relaxator) model considered by Debye [1] (and much extended by Fröhlich [49]), which is a Poisson-like process, where relaxation occurs due to rare members of an assembly of dipoles over a potential barrier by large jumps due to the shuttling action of thermal agitation. This model also produces a relaxation spectrum of the form of Eq. (69); however, the overbarrier relaxation time has Arrhenius-like behavior as it depends exponentially on the height of the potential barrier.

The Cole-Cole, Cole-Davidson, and Havriliak-Negami relaxation processes can be modeled via fractional diffusion equations by using the method of Nigmatullin and Ryabov [38]. According to this approach, the conventional kinetic equation describing the ac stationary response to a forcing function $F(t) = Fe^{i\omega t}$, namely,

$$\left(\tau_D \frac{d}{dt} + 1\right) f(t) = F(t), \tag{70}$$

for a system characterized by the single exponential relaxation function $f(t) = e^{-t/\tau_D}$ and, hence, the Debye equation for the complex susceptibility, Eq. (69), may be generalized to a fractional kinetic equation of fractional order α, so describing a system with Cole-Cole anomalous relaxation behavior as [44]

$$\left(\tau^{\alpha}_{D\,-\infty} D^{\alpha}_t + 1\right) f(t) = F(t), \tag{71}$$

where the fractional derivative ${}_{-\infty}D^{\alpha}_t$ is given by the Riemann-Liouville definition [39]

$${}_{-\infty}D^{\alpha}_t[f(t)] = \frac{1}{\Gamma(1-\alpha)} \frac{d}{dt} \int_{-\infty}^{t} \frac{f(t')dt'}{(t-t')^{\alpha}},$$

and $\Gamma(z)$ is the gamma function and $0 < \alpha < 1$. The physical meaning of the parameter α is the *fractal dimension* of the set of waiting times, which is the scaling of the waiting-time segments in the random walk with magnification. The fractional exponent α measures the statistical self-similarity (or how the whole looks similar to its parts) of the waiting time segments [40]. Assuming adiabatic switching on of the ac field $F(t) = Fe^{i\omega t}$, the solution of Eq. (71) yields the Cole-Cole Eq. (67). In the time domain, the exponential relaxation

function $f(t) = e^{-t/\tau_D}$ for the normal diffusion becomes $f(t) = E_\alpha[-(t/\tau_D)^\alpha]$ for anomalous relaxation, where $E_\alpha(z)$ is the Mittag-Leffler function defined as [39]

$$E_\alpha(z) = \sum_{n=0}^{\infty} \frac{z^n}{\Gamma(1+n\alpha)}.$$

The Mittag-Leffler function interpolates between the initial stretched exponential form $E_\sigma[-(t/\tau_D)^\alpha] \sim e^{-(t/\tau_D)^\alpha/\Gamma(1+\alpha)}$ and the long-time inverse power-law behavior $E_\sigma[-(t/\tau_D)^\alpha] \sim (t/\tau_D)^{-\alpha}/\Gamma(1-\alpha)$ [16]. In like manner, one may also introduce the fractional kinetic equation [40,42,44]

$$\left(\tau^\sigma {}_{-\infty}D_t^\alpha + 1\right)^\nu f(t) = F(t), \tag{72}$$

to incorporate the Havriliak-Negami anomalous relaxation. The fractional derivatives in Eqs. (71) and (72) are memory functions with a slowly decaying power law kernel in the time. Such behavior arises from random torques with an anomalous waiting time distribution.

The nonlinear dielectric and Kerr-effect relaxation, treated in the present paper via the rotational diffusion model, may be extended to anomalous relaxation by using the above fractional kinetic equation approach. Here we consider as an example the Cole-Cole relaxation mechanism characterizing by the anomalous exponent α (other relaxation mechanisms can be treated in like manner). The generalization of the theory, based on a fractional version of the Smoluchowski equation, namely,

$$\tau_D^{\alpha-1} {}_{-\infty}D_t^\alpha W = L_{\rm FP} W + L_t W, \tag{73}$$

has been fully explained in Refs. [16,44]. Here the general solution of Eq. (73) is of the form of the Fourier series, Eq. (6), so that, just as for the normal diffusion, we can obtain from Eq. (73) the fractional analogue of the differential-recurrence Eq. (9) for the response functions $f_n(t) = \langle P_n(\cos\vartheta)\rangle(t)$ [cf. Eq. (9)],

$$\begin{aligned}\left(\tau_{D\,-\infty}^\alpha D_t^\alpha + d_n\right) f_n(t) + c_n f_{n-2}(t) + g_n f_{n+2}(t) \\ = a_n(\xi_0 + \xi\cos\omega t)[f_{n-1}(t) - f_{n+1}(t)].\end{aligned} \tag{74}$$

Under linear response conditions, $\xi \ll 1$, and $\sigma, \xi_0 = 0$, Eq. (74) yields the linear susceptibility from Eq. (67). Moreover, just as for the normal diffusion, Eq. (74) also allows one to evaluate the nonlinear ac stationary responses via a generalization of the two-mode approximation (see Ref. [33] for details). In the time domain, such a two-mode approximation is equivalent to assuming that the relaxation function $\Phi_{nm}(t)$ may be approximated by *two* Mittag-Leffler functions only [cf. Eq. (35)],

$$\begin{aligned}\Phi_{nm}(t) \approx \Delta_{nm} E_\alpha[-(t/\tau_D)^\alpha \tau_D \lambda_1] \\ + (1-\Delta_{nm}) E_\alpha\left[-(t/\tau_D)^\alpha \tau_D/\tau_W^{(nm)}\right]\end{aligned} \tag{75}$$

(in general, $\Phi_{nm}(t)$ comprises an *infinite number* of Mittag-Leffler functions [44]). Noting that [16]

$$\int_0^\infty E_\sigma[-(t/\tau)^\alpha] e^{-st}\,dt = \frac{1}{s + \tau^{-\alpha} s^{1-\alpha}},$$

the corresponding normalized dynamic susceptibility $X_{nm}(\omega)$ may now be approximated by a sum of two Cole-Cole functions, viz.,

$$X_{nm}(\omega) \approx \frac{\Delta_{nm}}{1 + (i\omega/\omega_c)^\alpha} + \frac{1-\Delta_{nm}}{1 + \left(i\omega/\omega_W^{(nm)}\right)^\alpha}, \tag{76}$$

where $\omega_c = \tau_D^{-1}(\tau_D\lambda_1)^{1/\alpha}$ and $\omega_W^{(n1)} = \tau_D^{-1}(\tau_D/\tau_W^{(n1)})^{1/\alpha}$ are the characteristic frequencies. In particular, we have the generalization of Eqs. (65), viz.,

$$\begin{aligned}\overline{f_n}(\omega) \approx \langle P_n\rangle_0 + \frac{\chi_{n2}\xi^2}{2}\mathrm{Re}\left(\frac{\Delta_{n0}}{1 + (i\omega/\omega_c)^\alpha}\right. \\ \left. + \frac{1-\Delta_{n0}}{1 + \left(i\omega/\omega_W^{(n0)}\right)^\alpha}\right).\end{aligned} \tag{77}$$

All other nonlinear response equations obtained can be readily generalized in like manner. Such a generalization is likely to be important as the Cole-Cole relaxation behavior has proved useful in the analysis of magnetic and dielectric relaxation data.

IX. RESULTS AND DISCUSSION

We have presented two complementary approaches for treating the effects of an external dc bias field on the nonlinear ac stationary response of permanent dipoles in a uniaxial mean-field potential to any desired order of the ac field amplitude with arbitrary dc field strength. The first approach is based on perturbation theory, allowing one to calculate numerically the nonlinear ac stationary responses using powerful matrix methods. The results obtained from these numerical calculations are in complete agreement with the independent numerical solution of Ref. [23a] for weak ac fields, $\xi \ll 1$. The second, semianalytic approach, based on the two-mode approximation originally proposed to model linear response functions of dipolar systems [25,26], effectively generalizes the existing results to treat the nonlinear response of dipolar particles over wide ranges of the anisotropy and external field parameters. Our results apply both to nonlinear dielectric and Kerr-effect relaxation of nematic liquid crystals and to nonlinear magnetization relaxation and magnetic birefringence relaxation of magnetic nanoparticles. In particular, one may explain the successful application of the known frequency dependence of the Kerr-effect response for free rotational diffusion to the analysis of experimental spectra of electric birefringence of nematics, which was previously done without any theoretical justification (see, for example, Ref. [50]). Furthermore, the analytic solution for the Kerr-effect response (e.g., Figs. 1 and 3) clearly demonstrates that this response contains information about the longest relaxation time of the system, which is due to the overbarrier relaxation processes. This fact suggests that new methods of measurement of the overbarrier (longest) relaxation time are possible via the electric or magnetic birefringence. We remark that until now two kinds of nonlinear response experiments have usually been carried out, namely, where either (i) a strong ac field alone (for example, see Refs. [7,8]) or (ii) a weak ac field superimposed on a strong dc bias field (e.g., see Refs. [9,10]) was applied to the dielectric liquids. In polar dielectrics, although the applied fields in these experiments were high enough ($\geqslant 10^6$ V/m) to observe

nonlinear effects, their strengths were sufficiently weak to allow one to use the nonlinear response equations obtained using perturbation theory. Comparison of experimental data [7–10] with the perturbation theory results demonstrated that they are in agreement. However, as the theory presented here is also applicable for arbitrary dc field strengths, it provides a theoretical basis for comparison with nonlinear response experiments in high *dc* fields. Note that some molecular and Brownian dynamics simulation data for systems of dipolar molecules in strong ac fields are also available (e.g., see Refs. [51–56]). Furthermore, the use of computer simulation data is preferable to experimental data for testing a nonlinear theory as it is much easier to achieve high values of the dc field parameter $\xi_0 \geqslant 1$.

It is worth mentioning the experimental results of Wandersman *et al.* [57] in the context of the present work. In particular, these authors measured the magnetic birefringence in two dense ferrofluids. Their experimental data is fitted by the birefringence function

$$K(t) = ae^{-t/\tau_1} + (1-a)e^{-(t/\tau_2)^{\alpha}}, \tag{78}$$

where a is the normalized amplitude of the short-time decay mode and τ_1 is the associated time scale, while the τ_2 time scale describes the stretched exponential long time decay of the magnetic birefringence. Bearing in mind that this stretched exponential behaviour is the short time expansion of the Mittag-Leffler function, one may say that anomalous diffusion manifests itself at long times only. Equation (44) is then formally a special case of Eq. (78) with $\alpha = 1$. Equation (78) in turn suggests a straightforward generalization to fractional birefringence dynamics, which has been alluded to in Sec. VIII [see, for example, Eqs. (75) and (76)].

Now, as alluded to in the Introduction, Ladieu *et al.* [30] have recently suggested a model of nonlinear dielectric relaxation of supercooled liquids that has been compared with experimental data. The work presented here may be of importance in order to accurately represent their so-called "trivial" component (the words "trivial" component used by Ladieu and coworkers means a monotonic frequency behavior of the nonlinear response modulus, similar to the "ideal gas" behavior of the Coffey-Paranjape formulas [5], so that the nonlinear polarization response consists of this "trivial" component augmented by a "singular" component which must definitely be associated with intermolecular dynamical correlations). The formulas obtained in the present paper cannot describe all the features of the experimental spectrum, because dynamical correlations are not accounted for in the mean-field approximation. This is clearly illustrated by the quasimonotonic behavior of the moduli of the Fourier amplitudes for the nonlinear dielectric response, as can be seen in Fig. 7 (conversely, the moduli of the Fourier amplitudes for the Kerr-effect response have nonmonotonic behavior; see Fig. 8). However, the formulas presented here can be used in calculating quasi-static nonlinear properties of the polarization of glass-forming liquids, and therefore can be included in Ladieu's model [30] as a first approximation.

The given methods of the solution of infinite hierarchies of *multiterm* recurrence relations are quite general and can be applied to analogous nonlinear response problems, where time-dependent stimuli in high ac external fields are considered. In particular, our methods can also be used for the nonlinear dielectric and Kerr effect ac stationary responses of polar and *anisotropically polarizable* molecules [3,14]. Furthermore, they may be extended to nonstationary responses and to other mean-field potentials. Moreover, they can be applied (with small modifications) to the nonlinear magnetic response of uniaxial magnetic nanoparticles. Here the magnetization dynamics are governed by equations very similar to the

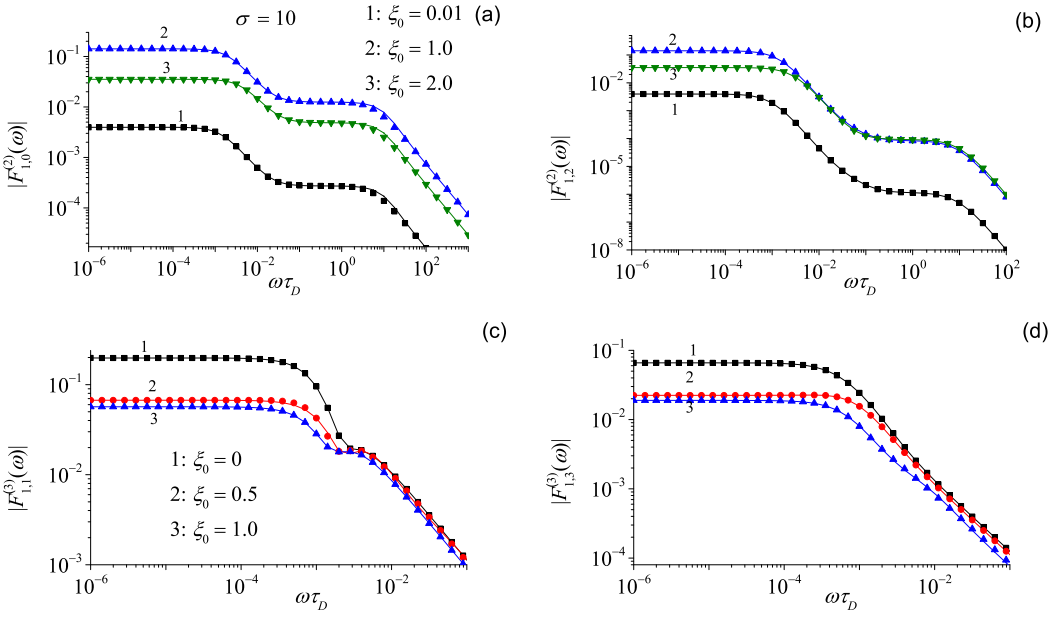

FIG. 7. Moduli of the dc component of the nonlinear dielectric response $|F^{(2)}_{1,0}(\omega)|$ (a), the second harmonic component of the nonlinear dielectric response $|F^{(2)}_{1,2}(\omega)|$ (b), the fundamental component of the nonlinear dielectric response $|F^{(3)}_{1,1}(\omega)|$ (c), and the third harmonic component of the nonlinear dielectric response $|F^{(3)}_{1,3}(\omega)|$ (d) vs. $\omega\tau_D$ for various dc field amplitudes ξ_0 with $\sigma = 10$. Solid lines: the matrix solution. Symbols: the two-mode approximation Eqs. (47), (48), (49), and (50) using fitting parameters.

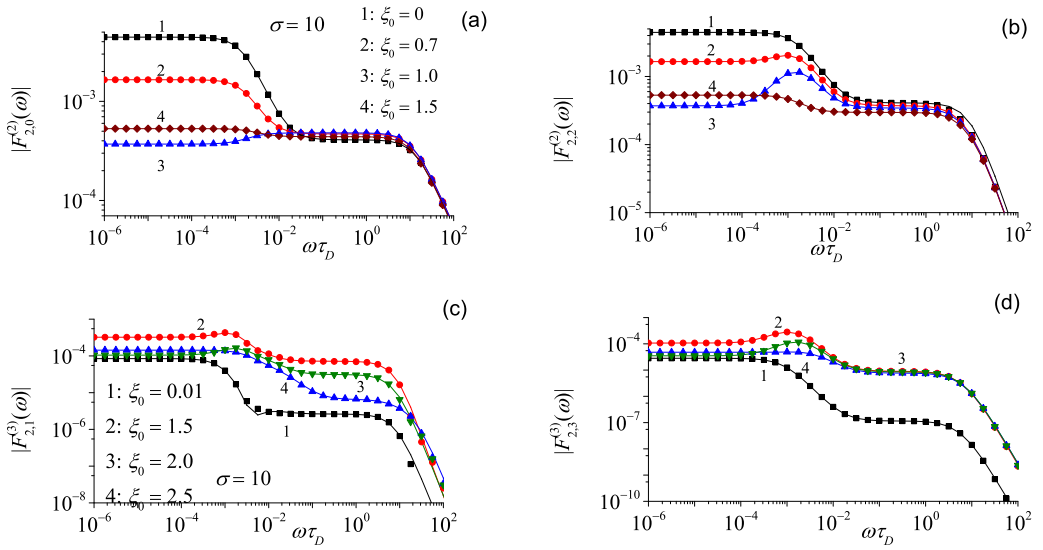

FIG. 8. Moduli of dc component of the second-order Kerr effect $|F^{(2)}_{2,0}(\omega)|$ (a), the Kerr effect second harmonic component $|F^{(2)}_{2,2}(\omega)|$ (b), the fundamental component of the third-order Kerr effect $|F^{(3)}_{2,1}(\omega)|$ (c), and the third harmonic component of the third-order Kerr effect $|F^{(3)}_{2,3}(\omega)|$ (d) vs. $\omega\tau_D$ for various dc field amplitudes ξ_0 with the anisotropy parameter $\sigma = 10$. Solid lines: the matrix solution. Symbols: the two-mode approximation Eqs. (39), (40), (58), and (59) using fitting parameters.

Fokker-Planck Eq. (2) [16,21,22]. Finally, the range of the area of applicability of the rotational diffusion model in the mean-field potential is restricted to the low-frequencies range ($\omega\tau_D \leqslant 1$), because the model does not include inertial effects. A consistent treatment of these effects must be carried out using the Fokker-Planck equation for the probability density function in configuration-angular velocity space. The inertia corrected rotational diffusion model in the uniaxial potential was used in Ref. [58] to determine the linear complex dielectric susceptibility tensor of polar liquid crystals in the entire frequency range of orientational polarization (up to 5 THz).

ACKNOWLEDGMENTS

We thank Dr. S.V. Titov and Dr. Byrne for helpful conversations. N. Wei also acknowledges the Studentship Award from Trinity College Dublin. Moreover, W. T. Coffey and N. Wei thank Ambassade de France en Irlande for research visits to Perpignan. P.M. Déjardin acknowledges stimulating scientific discussions with Dr. F. Ladieu.

APPENDIX A: STATIC SUSCEPTIBILITIES

In the case of superimposed ac and dc fields $\xi_0 + \xi\cos\omega t$ in the static limit, $\omega \to 0$, $f_n(0)$ to cubic order in ξ

$$f_n(0) = \frac{\int_{-1}^{1} P_n(x) e^{\sigma x^2+(\xi+\xi_0)x}dx}{\int_{-1}^{1} e^{\sigma x^2+(\xi+\xi_0)x}dx} = \frac{\langle P_n\rangle_0 + \xi\langle xP_n\rangle_0 + \frac{1}{2}\xi^2\langle x^2P_n\rangle_0 + \frac{1}{6}\xi^3\langle x^3P_n\rangle_0 + o(\xi^3)}{1 + \xi\langle x\rangle_0 + \frac{1}{2}\xi^2\langle x^2\rangle_0 + \frac{1}{6}\xi^3\langle x^3\rangle_0 + o(\xi^3)}$$

$$= \langle P_n\rangle_0 + \xi(\langle xP_n\rangle_0 - \langle x\rangle_0\langle P_n\rangle_0) + \xi^2\left[\frac{1}{2}(\langle x^2P_n\rangle_0 - \langle x^2\rangle_0\langle P_n\rangle_0) - \langle x\rangle_0(\langle xP_n\rangle_0 - \langle x\rangle_0\langle P_n\rangle_0)\right]$$

$$+\xi^3\left[\frac{1}{6}(\langle x^3P_n\rangle_0 - \langle x^3\rangle_0\langle P_n\rangle_0) + \langle x\rangle_0\langle P_n\rangle_0\left(\langle x^2\rangle_0 - \langle x\rangle_0^2\right) - \frac{1}{2}\langle x\rangle_0(\langle x^2P_n\rangle_0 - \langle x\rangle_0\langle xP_n\rangle_0) - \frac{1}{2}\langle xP_n\rangle_0\left(\langle x^2\rangle_0 - \langle x\rangle_0^2\right)\right]$$

$$+o(\xi^3). \tag{A1}$$

Because $P_1(x) = x$ and $P_2(x) = (3x^2 - 1)/2$, we have the first-, second-, and third-order contributions to $f_n(0)$, respectively,

$$f_n^{(1)}(0) = \xi\chi_{n1} = \xi(\langle P_1P_n\rangle_0 - \langle P_1\rangle_0\langle P_n\rangle_0), \tag{A2}$$

$$f_n^{(2)}(0) = \xi^2\chi_{n2} = \xi^2\left[\tfrac{1}{3}(\langle P_2P_n\rangle_0 - \langle P_2\rangle_0\langle P_n\rangle_0) - \langle P_1\rangle_0(\langle P_1P_n\rangle_0 - \langle P_1\rangle_0\langle P_n\rangle_0)\right], \tag{A3}$$

$$f_n^{(3)}(0) = \xi^3\chi_{n3} = \xi^3\left[\tfrac{1}{6}\left(\langle {P_1}^3P_n\rangle_0 - \langle {P_1}^3\rangle_0\langle P_n\rangle_0\right) + \langle P_1\rangle_0\langle P_n\rangle_0\left(\langle {P_1}^2\rangle_0 - \langle P_1\rangle_0^2\right)\right.$$

$$\left. - \tfrac{1}{2}\langle P_1\rangle_0\left(\langle {P_1}^2P_n\rangle_0 - \langle P_1\rangle_0\langle P_1P_n\rangle_0\right) - \tfrac{1}{2}\langle P_1P_n\rangle_0\left(\langle {P_1}^2\rangle_0 - \langle P_1\rangle_0^2\right)\right]. \tag{A4}$$

For the zero dc field case, $\xi_0 = 0$, the above results are dramatically simplify. Here, the odd $f_{2n-1}(0)$ are expressed via the stationary averages up to cubic order in ξ as

$$f_{2n-1}(0) = \xi\langle x P_{2n-1}\rangle_0 + \frac{\xi^3}{6}(\langle x^3 P_{2n-1}\rangle_0 - 3\langle x^2\rangle_0\langle x P_{2n-1}\rangle_0) + o(\xi^3)$$
$$= \xi\langle P_1 P_{2n-1}\rangle_0 + \frac{\xi^3}{30}\left[2\langle P_3 P_{2n-1}\rangle_0 - 3\left(5\left\langle P_1^2\right\rangle_0 + 1\right)\langle P_1 P_{2n-1}\rangle_0\right] + o(\xi^3). \tag{A5}$$

Similarly, the even $f_{2n}(0)$ up to second order in ξ are given by

$$f_{2n}(0) = \langle P_{2n}\rangle_0 + \frac{\xi^2}{2}(\langle x^2 P_{2n}\rangle_0 - \langle x^2\rangle_0\langle P_{2n}\rangle_0) + o(\xi^2)$$
$$= \langle P_{2n}\rangle_0 + \frac{\xi^2}{3}(\langle P_2 P_{2n}\rangle_0 - \langle P_2\rangle_0\langle P_{2n}\rangle_0) + o(\xi^2). \tag{A6}$$

APPENDIX B: TWO-MODE APPROXIMATION

In linear response theory [32,33], the normalized complex susceptibilities $X_{n1}(\omega)$ are defined via the normalized equilibrium correlation function $\Phi_{k,m}(t)$ via Eq. (31), where $\Phi_{k,m}(t)$ is defined as

$$\Phi_{km}(t) = \frac{\langle P_k(0)P_m(t)\rangle_0 - \langle P_k(0)\rangle_0\langle P_m(0)\rangle_0}{\langle P_k(0)P_m(0)\rangle_0 - \langle P_k(0)\rangle_0\langle P_m(0)\rangle_0}. \tag{B1}$$

Three time constants characterize the time behavior of $\Phi_{k,m}(t)$, namely the integral relaxation time τ_n is defined as the area under the decaying $\Phi_{n1}(t)$,

$$\tau_n = \int_0^\infty \Phi_{n1}(t)dt, \tag{B2}$$

the effective relaxation time $\tau_n^{\rm eff}$ describing the initial decay of $\Phi_{n1}(t)$ defined by

$$\tau_n^{\rm eff} = -\frac{1}{\dot\Phi_{n1}(0)}, \tag{B3}$$

and the longest relaxation time defined by the inverse of the smallest non-vanishing eigenvalue λ_1 of the Fokker-Plank operator $L_{\rm FP}$, which describes the slowest relaxation mode. Now, the low-frequency behavior of the normalized susceptibility $X_{n1}(\omega)$ is evaluated by taking the low-frequency limit $\omega \to 0$ in Eq. (31),

$$X_{n1}(\omega) = 1 - i\omega\int_0^\infty \Phi_{n1}(t)\,dt + \cdots = 1 - i\omega\tau_n + \cdots, \tag{B4}$$

while the high-frequency limit is obtained by taking the limit $\omega \to \infty$,

$$X_{n1}(\omega) = -\int_0^\infty \dot\Phi_{n1}(t)e^{-i\omega t}dt$$
$$= -\frac{\dot\Phi_{n1}(0)}{i\omega} + \cdots = -\frac{i}{\omega\tau_n^{\rm eff}} + \cdots. \tag{B5}$$

Thus, the low- and high-frequency behavior of $X_{n1}(\omega)$ is completely determined by the integral and effective relaxation times, respectively. Hence, the equivalent definitions of τ_n and $\tau_n^{\rm eff}$ can be given via Eqs. (B4) and (B5) as

$$\tau_n = \lim_{\omega\to 0}\frac{X_{n1}(0) - X_{n1}(\omega)}{i\omega},$$

$$\tau_n^{\rm eff} = -i\lim_{\omega\to\infty}\frac{1}{\omega X_{n1}(\omega)}. \tag{B6}$$

Here, the integral and effective relaxation times τ_n and $\tau_n^{\rm eff}$ are given by the exact analytic equations [16]

$$\tau_n = \frac{2\tau_D}{Z(\langle P_n P_1\rangle_0 - \langle P_n\rangle_0\langle P_1\rangle_0)}\int_{-1}^1 \frac{\psi_1(z)\psi_n(z)e^{\sigma z^2+\xi_0 z}}{1-z^2}dz, \tag{B7}$$

$$\tau_n^{\rm eff} = -\frac{1}{\dot\Phi_{n1}(0)} = \frac{\tau_D}{\chi_{n1}}[d_n\chi_{n1} + g_n\chi_{n+21} + c_n\chi_{n-21}$$
$$+ \xi_0 a_n(\chi_{n+11} - \chi_{n-11})], \tag{B8}$$

where

$$\psi_n(z) = \int_{-1}^z [P_n(x) - \langle P_n\rangle_0]e^{\sigma x^2+\xi_0 x}dx. \tag{B9}$$

The correlation function $\Phi_{n1}(t)$ generally comprises an infinity of relaxation modes (decaying exponentials), i.e., $\Phi_{n1}(t) = \sum_k c_k^n e^{-\lambda_k t}$; however, we can suppose $\Phi_{n1}(t)$ may be approximated by two modes only [25,26],

$$\Phi_{n1}(t) = \Delta_{n1}e^{-\lambda_1 t} + (1-\Delta_{n1})e^{-t/\tau_W^{(n1)}}, \tag{B10}$$

where the parameters Δ_{n1} and $\tau_W^{(n1)}$ given by

$$\Delta_{n1} = \frac{\tau_n/\tau_n^{\rm eff} - 1}{\lambda_1\tau_n - 2 + \left(\lambda_1\tau_n^{\rm eff}\right)^{-1}}, \tag{B11}$$

$$\tau_W^{(n1)} = \frac{\lambda_1\tau_n - 1}{\lambda_1 - 1/\tau_n^{\rm eff}}. \tag{B12}$$

Equations (B11) and (B12) are the solutions of algebraic equations due to substituting Eq. (36) into Eqs. (B4) and (B5), viz.,

$$\Delta_{n1}/\lambda_1 + (1-\Delta_n)\tau_W^{(n1)} = \tau_n.$$
$$\Delta_{n1}\lambda_1 + (1-\Delta_{n1})/\tau_W^{(n1)} = 1/\tau_n^{\rm eff} \tag{B13}$$

By inserting Eq. (B10) into Eq. (31), $\chi_{n1}(\omega)$ is obtained as the sum of two Lorentzians, Eq. (36).

APPENDIX C: PARAMETERS FOR THE TWO-MODE APPROXIMATION OF THE LINEAR DIELECTRIC AND KERR-EFFECT RESPONSES

To illustrate the results of Appendix B, we calculate explicitly the parameters appearing in Eq. (36) for the linear dielectric and Kerr-effect responses. For the dielectric response, the equations for τ_1 and $\tau_1^{\rm eff}$ required for the calculation of Δ_{11} and $\tau_W^{(11)}$ in Eq. (36) can be evaluated by letting $n=1$ in Eqs. (B8) and (B7), yielding Equation Section (Next)

$$\tau_1 = \frac{2\tau_D}{Z\left(\langle P_1^2\rangle_0 - \langle P_1\rangle_0^2\right)}\int_{-1}^{1}\frac{\psi_1^2(z)e^{\sigma(z^2+2hz)}}{1-z^2}dz, \tag{C1}$$

$$\tau_1^{\rm eff} = -\frac{1}{\dot\Phi_{11}(0)} = 2\tau_D\frac{\langle P_1^2\rangle_0 - \langle P_1\rangle_0^2}{1-\langle P_1^2\rangle_0}. \tag{C2}$$

Here the equilibrium averages $\langle P_1\rangle_0$ and $\langle P_1^2\rangle_0$ are, according to Eq. (16),

$$\langle P_1\rangle_0 = \frac{1}{Z}\int_{-1}^{1} x e^{\sigma(x^2+2hx)}dx = \frac{e^\sigma\sinh(2\sigma h)}{\sigma Z} - h, \tag{C3}$$

$$\begin{aligned}\langle P_1^2\rangle_0 &= \frac{1}{Z}\int_{-1}^{1} x^2 e^{\sigma(x^2+2hx)}dx\\ &= \frac{e^\sigma[\cosh(2\sigma h) - h\sinh(2\sigma h)]}{\sigma Z} + h^2 - \frac{1}{2\sigma},\end{aligned} \tag{C4}$$

where $h=\mu E_0/(2K)$ is the dimensionless dc bias field parameter, Z is the partition function given by

$$\begin{aligned}Z &= \int_{-1}^{1} e^{\sigma(x^2+2hx)}dx\\ &= \sqrt{\frac{\pi}{4\sigma}}e^{-\sigma h^2}\{\mathrm{erfi}[(1+h)\sqrt{\sigma}] + \mathrm{erfi}[(1-h)\sqrt{\sigma}]\},\end{aligned} \tag{C5}$$

and

$$\mathrm{erfi}(z) = \frac{2}{\sqrt{\pi}}\int_0^z e^{t^2}dt$$

is the error function of imaginary argument [31]. Now, in the low-barrier case, $\sigma, h \ll 1$, the behavior of λ_1, Δ_{11}, and $\tau_W^{(11)}$ is [16]

$$\begin{aligned}\lambda_1\tau_D = 1 &- \frac{2}{5}\sigma + \frac{48}{875}\sigma^2 - \frac{32}{21875}\sigma^3\\ &+ 4h^2\left(\frac{1}{10}\sigma^2 + \frac{1}{875}\sigma^3 + \cdots\right) + \cdots,\end{aligned} \tag{C6}$$

$$\frac{\tau_W^{(11)}}{\tau_D} = \frac{1}{6} + \frac{1}{135}\sigma + \left(\frac{175}{108} + \frac{1739}{486}\sigma + \cdots\right)h^2 + \cdots, \tag{C7}$$

$$\Delta_{11} = 1 - \frac{12}{4375}\sigma^2 - \frac{22}{375}\sigma^2h^2 + \cdots, \tag{C8}$$

respectively. Equation. (C6) is related to the smallest nonvanishing eigenvalue of the Fokker Planck operator, while Eqs. (C7) and (C8) may be evaluated by taking the Taylor series expansions of Eqs. (C1) and (C2) and then substituting the results into Eqs. (B11) and (B12). In the high-barrier case, $\sigma(1-h)^2 \gg 1$ and $h<1$, the behavior of λ_1, Δ_{11}, and $\tau_W^{(11)}$ is given by [16,26]

$$\begin{aligned}\lambda_1\tau_D \approx{}& \frac{(1-h^2)\sigma^{3/2}}{\sqrt{\pi}}\left[(1-h)\mathrm{e}^{-(1-h)^2\sigma} + (1+h)\mathrm{e}^{-(1+h)^2\sigma}\right]\\ &+\cdots,\end{aligned} \tag{C9}$$

$$\frac{\tau_D}{\tau_W^{(11)}} \approx 2(1+h)\sigma - \frac{5+h}{1+h} + \cdots, \tag{C10}$$

$$\Delta_{11} \approx \frac{1}{1+\frac{(1-h)\cosh^2(2\sigma h)}{4\sigma^2(1+h)^3}} + \cdots, \tag{C11}$$

where Eq. (C9) follows from asymptotic expansions of the mean first-passage time [1], while Eq. (C10) follows from Eq. (4.15) of Ref. [26] and Eq. (C11) can be evaluated from the partition function Z, Eq. (C5).

For the Kerr-effect response, the parameters Δ_{21} and $\tau_W^{(21)}$ are again expressed via three characteristic time constants, namely, the inverse of the smallest nonvanishing eigenvalue $1/\lambda_1$, the integral relaxation time τ_2 defined by Eq. (B7), and the effective relaxation time $\tau_2^{\rm eff}$ defined by Eq. (B8). The relaxation times τ_2 and $\tau_2^{\rm eff}$ are now given by Eqs. (B7) and (B8) for $n=2$. In the low barrier case, $\sigma \ll 1$, the behavior of Δ_{21}, and $\tau_W^{(21)}$ are given by, following the method for calculating Δ_{11} and $\tau_W^{(11)}$ [Eqs. (C7) and (C8)],

$$\begin{aligned}\frac{\tau_W^{(21)}}{\tau_D} &= \frac{1}{3} + \frac{1}{315}\sigma - \frac{1252}{165375}\sigma^2 - \frac{16}{315}\sigma^2h^2 + \cdots,\\ \Delta_{21} &= \frac{3}{4} - \frac{23}{280}\sigma + \frac{1149}{98000}\sigma^2 - \frac{11}{140}\sigma^2h^2 + \cdots,\end{aligned} \tag{C12}$$

while for the high-barrier case, $\sigma(1-h)^2 \gg 1$, we have the following relaxation times τ_2 and $\tau_2^{\rm eff}$:

$$\frac{\tau_2}{\tau_D} = \frac{8e^{\sigma(1-h)^2}\sqrt{\frac{\pi}{\sigma}}\left[1+\frac{\sinh(4\sigma h)}{4\sigma h}\right]^{-1}}{[1-h+e^{-4\sigma h}]\{2+4\sigma(1-h^2)^2 - e^{-\sigma(1-h)^2}[1+2\sigma(1+h)^2]\}}, \tag{C13}$$

$$\frac{\tau_2^{\rm eff}}{\tau_D} = 6h^2\frac{\cosh(4\sigma h)}{\sinh^2(4\sigma h)} + h\frac{64+28\sigma-7\cosh(4\sigma h)}{32\sigma\sinh(4\sigma h)} + (85+28\sigma)\frac{224\sigma^2h^2\cosh(8\sigma h)-1}{112\sigma^2\sinh^2(4\sigma h)}. \tag{C14}$$

Equations (C13) and (C14) can be used to evaluate $\tau_W^{(21)}$ and Δ_{21} for large σ in the range $h \leqslant 0.17$, since outside this range Eq. (C13) diverges exponentially from λ_1^{-1}. The parameters $\tau_W^{(21)}$ and Δ_{21} are then evaluated by Eqs. (B11) and (B12).

[1] P. Debye, *Polar Molecules* (Chem. Catalog. Co., New York, 1929).

[2] H. Benoit, Contribution à l'étude de l'effet Kerr présenté par les solutions diluées de macromolécules rigides, Ann. Phys. **6**, 561 (1951).

[3] H. Watanabe and A. Morita, Kerr effect relaxation in high electric fields, Adv. Chem. Phys. **56**, 255 (1984).

[4] A. Morita, On nonlinear dielectric relaxation, J. Phys. D: Appl. Phys. **11**, 1357 (1978).

[5] W. T. Coffey and B. V. Paranjape, Dielectric and Kerr effect relaxation in alternating electric fields, Proc. R. Ir. Acad. A **78**, 17 (1978).

[6] V. Rosato and G. Williams, Dynamic Kerr-effect and dielectric relaxation of polarizable dipolar molecules. Transient response including linear and non-linear effects, J. Chem. Soc. Faraday Trans. **277**, 1767 (1981).

[7] T. Furukawa, M. Tada, K. Nakajima, and I. Seo, Nonlinear dielectric relaxation in a vinylidene cyanide/vinyl acetate copolymer, Jpn. J. Appl. Phys. **27**, 200 (1988); T. Furukawa and K. Matsumoto, Nonlinear dielectric relaxation spectra for polyvinyle acetate, *ibid.* **31**, 840 (1992).

[8] C. Crauste-Thibierge, C. Brun, F. Ladieu, D. L'Hôte, G. Biroli, and J-P. Bouchaud, Evidence of Growing Spatial Correlations at the Glass Transition from Nonlinear Response Experiments, Phys. Rev. Lett. **104**, 165703 (2010); C. Brun, F. Ladieu, D. L'Hôte, M. Tarzia, G. Biroli, and J.-P. Bouchaud, Nonlinear dielectric susceptibilities: Accurate determination of the growing correlation volume in a supercooled liquid, Phys. Rev. B **84**, 104204 (2011).

[9] H. Block and E. F. Hayes, Dielectric behavior of stiff polymers in solution when subjected to high voltage gradients, Trans. Faraday. Soc. **66**, 2512 (1970).

[10] K. De Smet, L. Hellemans, J. F. Rouleau, R. Corteau, and T. K. Bose, Rotational relaxation of rigid dipolar molecules in nonlinear dielectric spectra, Phys. Rev. E **57**, 1384 (1998); P. Kędziora, J. Jadżyn, K. De Smet, and L. Hellemans, Linear and nonlinear dipolar relaxation of 4,4′-n-hexylcyanobiphenyl, J. Mol. Liquids **80**, 19 (1999); J. Jadżyn, P. Kędziora, and L. Hellemans, Frequency dependence of the nonlinear dielectric effect in diluted dipiolar solutions, Phys. Lett. A **251**, 49 (1999); P. Kędziora, J. Jadżyn, K. De Smet, and L. Hellemans, Nonlinear dielectric relaxation in non-interacting dipolar systems, Chem. Phys. Lett. **289**, 541 (1998).

[11] Yu. L. Raikher, V. I. Stepanov, and S. V. Burylov, Nonlinear orientation-optical effects in a dipolar particle suspension, Kolloid. Zh., **52**, 887 (1990) [Colloid J. USSR, **52**, 768 (1990)]; Low-frequency dynamics of the orientational birefringence in a suspension of dipolar particles, J. Coll. Interface Sci., **144**, 308 (1991).

[12] J. L. Déjardin and Yu. P. Kalmykov, Nonlinear dielectric relaxation of polar molecules in a strong ac electric field: Steady state response, Phys. Rev. E **61**, 1211 (2000); Steady state response of the nonlinear dielectric relaxation and birefringence in strong superimposed ac and dc bias electric fields: Polar and polarizable molecules, J. Chem. Phys. **112**, 2916 (2000); Yu. P. Kalmykov, Matrix method of calculation of the Kerr effect transient and ac stationary responses of arbitrarily shaped macromolecules, *ibid.* **131**, 074107 (2009).

[13] J. L. Déjardin, Y. P. Kalmykov, and P. M. Déjardin, Birefringence and dielectric relaxation in strong electric fields, Adv. Chem. Phys. **117**, 275 (2001).

[14] R. B. Jones, Transient and steady linear response of dielectric particles in a high bias field subject to a weak AC probe field, J. Phys.: Condens. Matter, **14**, 7719 (2002); B. U. Felderhof and R. B. Jones, Nonlinear response of a dipolar system with rotational diffusion to an oscillating field, *ibid.* **15**, S1363 (2003); Mean field theory of the nonlinear response of an interacting dipolar system with rotational diffusion to an oscillating field, *ibid.* **15**, 4011 (2003).

[15] R. Richert, Frequency dependence of dielectric saturation, Phys. Rev. E **88**, 062313 (2013).

[16] W. T. Coffey and Yu. P. Kalmykov, *The Langevin Equation*, 3rd ed. (World Scientific, Singapore, 2012).

[17] G. Meier and A. Saupe, Dielectric relaxation in nematic liquid crystals, Mol. Cryst. **1**, 515 (1966); A. J. Martin, G. Meier, and A. Saupe, Extended Debye theory for dielectric relaxation in nematic liquid crystals, Symp. Faraday Soc. **5**, 119 (1971); P. L. Nordio, G. Rigatti, and U. Segre, Dielectric relaxation theory in nematic liquids, Mol. Phys. **25**, 129 (1973); B. A. Storonkin, Theory of dielectric relaxation in nematic liquid crystals, Kristallografiya **30**, 841 (1985); [Sov. Phys. Crystallogr. **30**, 489 (1985)]; A. Kozak, J. K. Moscicki, and G. Williams, On dielectric relaxation in liquid crystals, Mol. Cryst. Liq. Cryst. **201**, 1 (1991).

[18] W. T. Coffey, D. S. F. Crothers, Y. P. Kalmykov, and J. T. Waldron, Exact solution for the extended Debye theory of dielectric relaxation of nematic liquid crystals, Physica A **213**, 551 (1995); Yu. P. Kalmykov and W. T. Coffey, Analytical solutions for rotational diffusion in the mean field potential: application to the theory of dielectric relaxation in nematic liquid crystals, Liquid Cryst. **25**, 329 (1998); W. T. Coffey and Yu. P. Kalmykov, Rotational diffusion and dielectric relaxation in nematic liquid crystals, Adv. Chem. Phys. **113**, 487 (2000).

[19] P. M. Déjardin, Magnetic relaxation of a system of superparamagnetic particles weakly coupled by dipole-dipole interactions, J. Appl. Phys. **110**, 113921 (2011); P. M. Déjardin and F. Ladieu, Nonlinear susceptibilities of interacting polar molecules in the self-consistent field approximation, J. Chem. Phys. **140**, 034506 (2014).

[20] J. Jadzyn, G. Czechowski, R. Douali, and C. Legrand, On the molecular interpretation of the dielectric relaxation of nematic liquid crystals, Liquid Cryst. **26**, 1591 (1999); S. Urban, A. Würflinger, and B. Gestblom. On the derivation of the nematic order parameter from the dielectric relaxation time, Phys. Chem. Chem. Phys. **1**, 2787 (1999); S. Urban, B. Gestblom, W. Kuczyński, S. Pawlus, and A. Würflinger, Nematic order parameter as determined from dielectric relaxation data and other methods, *ibid.* **5**, 924 (2003); S. Urban, B. Gestblom, and S. Pawlus, Dielectric properties of 4-methoxy-4'-cyanobiphenyl (1 OCB) in the supercooled isotropic and nematic phases, Z. Naturforsch. A, **58**, 357 (2003); K. Merkel, A. Kocot, J. K. Vij, G. H. Mehl, and T. Meyer, Orientational order and dynamics of the dendritic liquid crystal organo-siloxane tetrapodes determined using dielectric spectroscopy, Phys. Rev. E **73**, 051702 (2006).

[21] W. F. Brown, Jr., Thermal fluctuations of a single-domain particle, Phys. Rev. **130**, 1677 (1963).

[22] Yu. L. Raikher and V. I. Stepanov, Nonlinear dynamic susceptibilities and field-induced birefringence in magnetic particle assemblies, Adv. Chem. Phys. **129**, 419 (2004); I. S. Poperechny, Yu. L. Raikher, and V. I. Stepanov, Dynamic magnetic hysteresis in single-domain particles with uniaxial anisotropy, Phys. Rev. B **82**, 174423 (2010).

[23] P. M. Déjardin and Yu. P. Kalmykov, Relaxation of the magnetization in uniaxial single-domain ferromagnetic particles driven by a strong ac magnetic field, J. Appl. Phys. **106**, 123908 (2009); S. V. Titov, P. M. Déjardin, H. El Mrabti, and Yu. P. Kalmykov, Nonlinear magnetization relaxation of superparamagnetic nanoparticles in superimposed ac and dc magnetic bias fields, Phys. Rev. B **82**, 100413(R) (2010); H. El Mrabti, S. V. Titov, P. M. Déjardin, and Yu. P. Kalmykov, Nonlinear stationary ac response of the magnetization of uniaxial superparamagnetic nanoparticles, J. Appl. Phys. **110**, 023901 (2011); N. Wei, D. Byrne, W. T. Coffey, Yu. P. Kalmykov, and S. V. Titov, Nonlinear frequency-dependent effects in the dc magnetization of uniaxial magnetic nanoparticles in superimposed strong alternating current and direct current fields, *ibid.* **116**, 173903 (2014).

[24] W. T. Coffey, D. S. F. Crothers, Yu. P. Kalmykov, and P. M. Déjardin, Nonlinear response of permanent dipoles in a uniaxial potential to alternating fields, Phys. Rev. E **71**, 062102 (2005); W. T. Coffey, D. S. F. Crothers, and Yu. P. Kalmykov, Nonlinear response of permanent dipoles in a mean-field potential to alternating fields, J. Noncryst. Solids **352**, 4710 (2006).

[25] W. T. Coffey, Y. P. Kalmykov, and N. Wei, Nonlinear normal and anomalous response of non-interacting electric and magnetic dipoles subjected to strong AC and DC bias fields, Nonlinear Dyn. **80**, 1861 (2014).

[26] D. A. Garanin, Integral relaxation time of single-domain ferromagnetic particles, Phys. Rev. E **54**, 3250 (1996)

[27] Y. P. Kalmykov, W. T. Coffey, and S. V. Titov, Analytic calculation of the longitudinal dynamic susceptibility of uniaxial superparamagnetic particles in a strong uniform dc magnetic field, J. Magn. Magn. Mater. **265**, 44 (2003).

[28] A. Morita, Theory of nonlinear response, Phys. Rev. A **34**, 1499 (1986); A. Morita and H. Watanabe, Nonlinear response and its behavior in transient and staionary processes, *ibid.* **35**, 2690 (1987).

[29] D. L'Hôte, R. Tourbot, F. Ladieu, and P. Gadige, Control parameter for the glass transition of glycerol evidenced by the static field-induced nonlinear response, Phys. Rev. B **90**, 104202 (2014).

[30] F. Ladieu, D. l'Hôte, and C. Brun, Nonlinear dielectric susceptibilities in supercooled liquids: A toy model, Phys. Rev. B **85**, 184207 (2012).

[31] *Handbook of Mathematical Functions*, edited by M. Abramowitz and I. Stegun (Dover, New York, 1965).

[32] R. Bellman, *Introduction to Matrix Analysis* (McGraw-Hill, New York, 1960).

[33] R. Kubo, M. Toda, and N. Hashitsume, *Statistical Physics II, Non-Equilibrium Statistical Mechanics*, 2nd ed. (Springer-Verlag, Berlin, 1991).

[34] H. Risken, *The Fokker-Planck Equation*, 2nd ed. (Springer, Berlin, 1989).

[35] S. Havriliak and S. Negami, A complex plane representation of dielectric and mechanical relaxation processes in some polymers, Polymer **8**, 161 (1967).

[36] K. S. Cole and R. H. Cole, Dispersion and absorption in dielectrics. I. Alternating current characteristics, J. Chem. Phys. **9**, 341 (1941).

[37] D. W. Davidson and R. H. Cole, Dielectric relaxation in glycerol, propylene glycol, and n-Propanol, J. Chem. Phys. **19**, 1484 (1951).

[38] R. R. Nigmatullin and Ya. A. Ryabov, Cole–Davidson dielectric relaxation and self-similar relaxation process, Fiz. Tverd. Tela (St. Petersburg) **39**, 101 (1997) [Phys. Solid State **39**, 87 (1997)].

[39] R. Metzler and J. Klafter, The random walk's guide to anomalous diffusion: A fractional dynamics approach, Phys. Rep. **339**, 1 (2000).

[40] V. V. Novikov and V. P. Privalko, Temporal fractal model for the anomalous dielectric relaxation of inhomogeneous media with chaotic structure, Phys. Rev. E **64**, 031504 (2001).

[41] R. Hilfer, H-function representations for stretched exponential relaxation and non-Debye susceptibilities in glassy systems, Phys. Rev. E **65**, 061510 (2002).

[42] W. T. Coffey, Yu. P. Kalmykov, and S. V. Titov, Anomalous dielectric relaxation in the context of the Debye model of non-inertial rotational diffusion, J. Chem. Phys. **116**, 6422 (2002); Yu. P. Kalmykov, D. S. F. Crothers, W. T. Coffey, and S. V. Titov, Microscopic models for dielectric relaxation in disordered systems, Phys. Rev. E **70**, 041103 (2004).

[43] E. Gudowska-Nowak, K. Bochenek, A. Jurlewicz, and K. Weron, Hopping models of charge transfer in a complex environment: Coupled memory continuous-time random walk approach, Phys. Rev. E **72**, 061101 (2005).

[44] W. T. Coffey, Yu. P. Kalmykov, and S. V. Titov, Fractional rotational diffusion and anomalous dielectric relaxation in dipole systems, Adv. Chem. Phys. B **133**, 285 (2006).

[45] I. Goychuk, Anomalous relaxation and dielectric response, Phys. Rev. E **76**, 040102 (2007).

[46] W. T. Coffey, Yu. P. Kalmykov, and S. V. Titov, Anomalous nonlinear dielectric and Kerr effect relaxation steady state responses in superimposed ac and dc electric fields, J. Chem. Phys. **126**, 084502 (2007).

[47] V. V. Uchaikin and R. T. Sibatov, *Fractional Kinetics in Solids: Anomalous Charge Transport in Semiconductors, Dielectrics and Nanosystems* (World Scientific Publishing Company, Singapore, 2012).

[48] A. A. Khamzin, R. R. Nigmatullin, and I. I. Popov, Log-periodic corrections to the Cole–Cole expression in dielectric relaxation, Physica A **392**, 136 (2013).

[49] H. Fröhlich, *Theory of Dielectrics*, 2nd ed. (Oxford University Press, Oxford, 1958).

[50] M. Schadt, Kerr effect and orientation relaxation of pre-transitional domains and individual molecules in positive dielectric liquid crystals, J. Chem. Phys. **67**, 210 (1977).

[51] M. W. Evans, Computer simulation of liquid anisotropy. III. Dispersion of the induced birefringence with a strong alternating field, J. Chem. Phys. **77**, 4632 (1982); Computer simulation of some field-induced phenomena of molecular liquids, J. Mol. Liquids **26**, 49 (1983).

[52] J. Antosiewicz and D. Porschke, Brownian dynamics simulation of electrooptical transients for complex macrodipoles, J. Phys. Chem. **97**, 2767 (1993); D. Porschke and J. Antosiewicz, Strong effect of hydrodynamic coupling on the

electric dichroism of bent rods, J. Phys. Chem. B **109**, 1034 (2005).

[53] B. C. Gómez, A. P. Belmonte, M. C. L. Martínez, and J. G. de la Torre, Transient orientation and electrooptical properties of axially symmetric macromolecules in an electric field of arbitrary strength, J. Phys. Chem. **100**, 9900 (1996).

[54] M. X. Fernandes and J. G. de la Torre, Brownian dynamics simulation of rigid particles of arbitrary shape in external fields, Biophys. J. **83**, 3039 (2002).

[55] J. G. de la Torre, Dynamic electro-optic properties of macromolecules and nano-particles in solution: A review of computational and simulation methodologies, Colloids and Surfaces B: Biointerfaces **56**, 4 (2007).

[56] T. R. Evensen, S. N. Naess, and A. Elgsaeter, Use of the rotation vector in Brownian dynamics simulation of transient electro-optical properties, Macromol. Theory Simul. **18**, 50 (2009).

[57] E. Wandersman, V. Dupuis, E. Dubois, and R. Perzynski, Phys. Rev. E **80**, 041504 (2009).

[58] Yu. P. Kalmykov, S. V. Titov, and W. T. Coffey, Inertial and bias effects in the rotational Brownian motion of rodlike molecules in a uniaxial potential, J. Chem. Phys. **134**, 044530 (2011).